Carcinogenesis vol.29 no.2 pp.418–426, 2008
doi:10.1093/carcin/bgm225
Advance Access publication January 3, 2008

A novel *ras*H2 mouse carcinogenesis model that is highly susceptible to 4-NQO-induced tongue and esophageal carcinogenesis is useful for preclinical chemoprevention studies

Shingo Miyamoto, Yumiko Yasui[1], Mihye Kim, Shigeyuki Sugie[1], Akira Murakami, Rikako Ishigamori-Suzuki[1] and Takuji Tanaka*

Division of Food Science and Biotechnology, Graduate School of Agriculture, Kyoto University, Kyoto 606-8502, Japan and [1]Department of Oncologic Pathology, Kanazawa Medical University, 1-1 Daigaku, Uchinada, Ishikawa 920-0293, Japan

*To whom correspondence should be addressed. Tel: +81 76 218 8116; Fax: +81 76 286 6926; Email: takutt@kanazawa-med.ac.jp

We investigated the susceptibility of 4-nitroquinoline 1-oxide (4-NQO)-induced tongue carcinogenesis in male CB6F1-Tg-*ras*H2 @Jcl mice (Tg mice). The Tg mice were administered 4-NQO (20 p.p.m. in drinking water) for 2, 4, 6 or 8 weeks, and thereafter they were untreated up to week 24. At week 24, a higher incidence (80%) of tongue neoplasm with dysplasia was noted in the mice that received 4-NQO for 8 weeks in comparison with the other groups (20% incidence for each) treated with 4-NQO for 2, 4 and 6 weeks. Esophageal tumors also developed in the Tg mice were 4-NQO. Immunohistochemical observation revealed that the EP receptors, especially EP_1 and EP_2, expressed in the tongue and esophageal lesions induced by 4-NQO, thus suggesting the involvement of prostaglandin (PG) E_2 and $EP_{1,2}$ receptors in the tongue and esophageal carcinogenesis. Using this animal model, we investigated the potential chemopreventive ability of pitavastatin (1, 5 and 10 p.p.m. in diet for 15 weeks), starting 1 week after the cessation of 4-NQO-exposure (20 p.p.m. in drinking water for 8 weeks). Dietary pitavastatin at 10 p.p.m. significantly reduced the incidence and multiplicity of the tongue, but not esophageal neoplasms by the modulation of prostaglandin E2 biosynthesis, EP_1 and EP_2 expression and proliferation. Our results thus suggest that a *ras*H2 mouse model of 4-NQO-induced tongue and esophageal carcinogenesis can be utilized for investigating the pathogenesis of cancer development in these tissues and may well prove to be useful for identifying candidate cancer chemopreventive agents for the upper digestive organs.

Introduction

Oral cancer is the 11th most common human neoplasm and accounts for 3% of all newly diagnosed cancers (1). While this epithelial malignancy mainly developed in the elderly in the past, an increased number of young patients with oral malignancy being seen at present in Europe, North America and India are increased today (2,3). Such prevalence is largely associated with the habit of using chewing tobacco and other related products. More than 90% of oral cancers are histopathologically squamous cell carcinomas (SCCs) (4), with >300 000 new cases being diagnosed every year worldwide (5). Despite efforts to improve the overall outcome, the survival rates of oral cancer patients have not changed for the last 20 years. Since ~50 to 70% of patients die within 5 years due to local recurrence, invasion or metastasis in the esophagus and/or lung, or second primary cancers, generally elsewhere in the oral cavity ('field cancerization' theory) (6–8), the prognosis is poor. The detection of many cancers including oral cancer is often too late for successful intervention. Therefore, if appropriate biological markers can identify pre-malignant lesions, then we can detect them and prevent cancer development before they progress to malignancies by the use of chemoprevention modalities or other therapeutics (9,10). The incidence rates for one of the oral pre-malignant lesions, leukoplakia with dysplastic nature, in the Japanese are somewhat higherthan those reported from India, since the risk habits of the two countries are both markedly different (11).

The development of oral cancer is a multistep process, which includes hyperplasia, dysplasia and finally neoplasm (benign and malignant) (10). During these steps, the accumulation of genetic alterations, including chromosomal aberrations, DNA mutations, amplifications or deletions and/or epigenetic alterations (methylation) occur (12–15). These events are often influenced by exposure to environmental agents. These include tobacco smoke, alcohol beverages and viruses as the major risk factors (10). In patients, the analysis of these events during the multistep process is hampered by the unavailability of biopsies obtained at all stages (namely hyperplasia, dysplasia and neoplasm) of carcinogenesis. However, animal models of oral carcinogenesis allow the reproducible isolation of all stages, including normal tissues, which are then amenable to pathological, genetic and biochemical analyses. Thus, appropriate animal models are essential for investigating the transition of oral squamous epithelium from normal through dysplastic states and ultimately into SCC. There are several animal models for oral carcinogenesis (16). Among them, the systemic application of 4-nitroquinoline 1-oxide (4-NQO) via drinking water is easily able to induce tongue tumors in rats (10,17) and mice (18). Recent reviews (5,19) have concluded that the rat 4-NQO-induced tongue carcinogenesis is the main model for simulating the process of oral carcinogenesis in humans with a fair degree of reliability. However, in contrast to rats (10), oral and esophageal tumors develop in mice that receive 4-NQO in drinking water (18). This suggests that a mouse model initiated with 4-NQO is useful for investigating field cancerization in the regions (8).

H-*ras* mutations are implicated in human and murine oral carcinogenesis (20–22). *Ras* mutations are observed in oral cancer with different frequencies in different countries (20,23). Our recent findings suggest that human c-Ha-*ras* proto-oncogene-carrying transgenic rats are highly susceptible to a water-soluble carcinogen 4-NQO in their tongue (24), thus suggesting an excellent rat model for investigating oral cancer development and treatment/chemoprevention of this malignancy. Few studies, nevertheless, have addressed the aspect of *ras* activation, while considering its possible role in mouse oral carcinogenesis. CB6F1-Tg *ras*H2@Jcl mice (Tg mice) were developed by Saitoh *et al.* (25) to evaluate the association of chemically induced transgene expression and tumor induction (26,27). Three copies of the human transgene were integrated into the mouse genome in a tandem array through pronuclear injection. The Tg mice are hemizygous for the human c-Ha-*ras* transgene under control of its endogenous promoter and enhancer sequences. Expression of the transgenic protein is observed in normal tissues and increased ~2-fold in chemically induced tumors (28). Mutation of the endogenous mouse ras genes or of the transgene is infrequent and unpredictable.

Prostaglandins (PGs) are generated via the cyclooxygenase (COX)-1 and -2 and are known to be elevated in the rat tongue following 4-NQO exposure (29). COX-1 and COX-2 both catalyze the first reaction in the conversion of arachidonic acid into PGs, of which prostaglandin E_2 (PGE_2) is the major product found in the rat tongue exposed to 4-NQO (29). COX-1 is the constitutively expressed isoform, and COX-2 is the inducible isoform (30). Although a number of studies indicate that the inhibition of PGE_2 biosynthesis through COX-2 expression contributes to the suppression of cancer development in a variety of tissues (31), including tongue cancer (24,32). COX-2 deregulation is reported in smokeless tobacco-related oral

Abbreviations: COX, cyclooxygenase; PAP, squamous cell papilloma; PBS, phosphate buffer saline; PCNA, proliferative cell nuclear antigen; PG, prostaglandin; PGE_2, prostaglandin E_2; SCC, squamous cell carcinoma; 4-NQO, 4-nitroquinoline 1-oxide.

carcinogenesis (33,34). COX-1 is also involved in carcinogenesis in the colon (35,36) and the tongue (T. Tanaka, Y. Yasui, M. Kim, in preparation). Therefore, both isoforms are involved in carcinogenesis (37). PGE_2 manifests its biological activities through four known G-protein-coupled membrane receptors, EP_1, EP_2, EP_3 and EP_4 (38). Recently reported findings suggest that these PGE_2 receptors contribute to murine tumorigenesis in the colon (37), skin (39) and mammary gland (40). We have recently reported that an EP_1-selective antagonist, ONO-8711, can effectively inhibit 4-NQO-induced tongue carcinogenesis in rats (41), thus suggesting that certain EP receptors are involved in chemically induced tongue carcinogenesis. However, detailed investigations on the expression of all EP receptors are scarce.

In the current study, we investigated the susceptibility of 4-NQO-induced tongue carcinogenesis in male Tg mice to inspect our previous finding that the tongue of human c-Ha-*ras* proto-oncogene-carrying transgenic rats is highly susceptible to 4-NQO-induced carcinogenesis. In addition, we immunohistochemically examined the different expression of four EP receptors in normal squamous epithelium, in dysplasia and in neoplasms in the tongue of Tg mice that are adequately evaluated for consideration for carcinogenicity testing of pharmaceutical candidates (42). Subsequently, the chemopreventive potential of a lipophilic statin, pitavastatin (43), against 4-NQO-induced carcinogenesis in the Tg mice was investigated to determine whether this animal model can be utilized for preclinical animal studies for cancer chemoprevention. Pitavastatin affects the expression of $p21^{waf1}$ that is involved in oral cancer development (21,44), and ras p21 is a target for cancer chemoprevention by statins (45). In addition, pitavastatin is able to inhibit NAD(P)H oxidase activity (46), which is involved in 4-NQO-induced mutagenicity, carcinogenicity and oxidative stress (47). Statins modulate PGs biosynthesis and downregulate COX-2 expression (48). We thus suspected that pitavastatin affects oral carcinogenesis in the Tg mice treated with 4-NQO.

Materials and methods

Animals, diets and carcinogen

Male CB6F1-Tg *ras*H2@Jcl mice (Tg) and non-Tg males bred by CLEA Japan (Tokyo, Japan) at 6 weeks of age were obtained and maintained in plastic cages in an experimental room controlled at 23 ± 2°C temperature, 50 ± 10% humidity and lighting (12 h light/dark cycle). They were all allowed free access to a powdered basal diet of CRF (Charles River Formula)-1 (Oriental Yeast Co., Ltd, Tokyo, Japan) and to tap water. The experiments were conducted according to the 'Guidelines for Animal Experiments in Kanazawa Medical University'. A carcinogen, 4-NQO (98% pure, CAS no. 56-57-5, Wako Pure Chemical Ind., Osaka, Japan) was used to induce tongue and/or esophageal tumors in this study.

Experimental procedure for developing the rasH2 tongue and esophageal carcinogenesis model

A total of 22 Tg and 24 non-Tg male mice were transferred to the experimental room after a 1 week quarantine. They were given tap water containing 20 p.p.m. 4-NQO for 2 (group 1, $n = 5$, each of Tg and non-Tg mice), 4 (group 2, $n = 5$, each of Tg and non-Tg mice), 6 (group 3, $n = 5$, each of Tg and non-Tg mice) and 8 weeks (group 4, $n = 5$, each of Tg and non-Tg mice), and thereafter they received no further treatments. Two *ras*H2 mice (group 5) and four non-Tg mice (group 5) were untreated controls. The animals were killed at 24 weeks to determine the occurrence of preneoplasms and neoplasms in the tongue and esophagus. At killing by exsanguination under a deep ether anesthesia, macroscopic observations were carefully performed and the numbers of grossly visible tumors in the tongue and esophagus were recorded, and then these tissues with or without tumors were processed for histopathological examination after being fixed in 10% buffered formalin. The tongues and esophagus with or without lesions were also processed to assess the expression of EP receptors and a cell proliferation biomarker by immunohistochemistry. For a histological examination, the tissue and gross lesions were fixed in 10% buffered formalin, embedded in paraffin blocks and then the histological sections were stained with hematoxylin and eosin. Epithelial lesions (dysplasia and neoplasia) in both tissues were diagnosed according to the criteria described by Kramer *et al.* (49). To determine the multiplicity of the tongue and esophageal lesions, the tissue specimens were examined for gross lesions without the use of any magnification aid. Tissue specimens from both the tongue and esophagus were cut in half longitudinally and each tissue specimen was fixed in 10% buffered formalin. Each tissue specimen was totally submitted as multiple transverse sections for histological processing. This averaged 5–6 pieces/tissue specimen of the tongue and 10–12 pieces/tissue specimen of the esophagus. The lesions in the tissues were counted on all slides stained with hematoxylin and eosin, and then the sum was divided by the number of slides, and they were expressed as the mean ± SD.

Immunohistochemistry of EP receptors

An immunohistochemical analysis of the EP receptors, EP_{1-4}, of the tongue and esophagus specimens from all the mice was done. Four-micrometer-thick paraffin sections of the 10% buffered formalin-fixed tongue and esophagus were mounted on salinized glass and deparaffinized in xyline and descending strengths of ethanol. The sections were washed in 0.05 M phosphate buffer saline (PBS, pH 7.6). The endogenous peroxidase activity and non-specific binding were blocked by incubations with 0.3% hydrogen peroxide in methanol for 5 min at room temperature. After being rinsed with PBS three times for 9 min and exposed to PBS/1% bovine serum albumin for 5 min at room temperature to reduce non-specific binding, the slides were incubated overnight at 4°C with rabbit polyclonal antibodies against EP_1 (code no. 101740, Cayman Chemical Co., Ann Arbor, MI), EP_2 (code no. 101760, Cayman Chemical Co.), EP_3 (code no. 101750, Cayman Chemical Co.) and EP_4 (code no. 101775, Cayman Chemical Co.), all being diluted at 1:1500 in PBS. The slides were rinsed three times for 9 min in PBS and incubated for 30 min in Dako Envision+ Peroxidase Rabbit (K4003, Dako Japan, Kyoto, Japan). The slides were rinsed three times for 9 min in PBS. Thereafter, they were incubated for 1 min in 3,3′-diaminobenzidine-4HCl and rinsed with PBS. Finally, the sections were counterstained with Mayer's hematoxylin. The negative controls were prepared by substituted primary antibody with buffered saline. To estimate the degree of stainability of the EP receptors in the lesions, the grading system (grade 0–5) was used: grade 0–10, no immunoreactivity; grade 1, very weak immunoreactivity in 11–20% of cells; grade 2, weak immunoreactivity in 21–30% of cells; grade 3, weak immunoreactivity in 31–40% of cells; grade 4, moderate immunoreactivity in 41–50% of cells and grade 5, marked immunoreactivity in 51–100% of cells. The results of the immunohistochemical analysis were blindly scored as a 'normal' appearing squamous epithelium, severe dysplasia, squamous cell papilloma (PAP) and SCC that developed in all groups.

Preclinical chemoprevention study of pitavastatin using rasH2 male mice

Since no tumors developed in the tongue and esophagus of non-Tg mice, a preclinical chemoprevention study for evaluating possible inhibitory effects of pitavastatin on 4-NQO-induced tumorigenesis was conducted in male Tg mice. Forty-two Tg males were divided into six experimental and control groups. Groups 1 through 4 were given 4-NQO (20 p.p.m. in drinking water) for 8 weeks. Group 1 received no further treatment. Starting 1 week after the cessation of 4-NQO exposure, animals in groups 2, 3 and 4 were fed the diets containing pitavastatin at dose levels of 1, 5 and 10 p.p.m. for 15 weeks, respectively. Group 5 was given the diet mixed with 10 p.p.m. pitavastatin. Group 6 was an untreated control. At week 24, all mice were killed by exsanguination under deep ether anesthesia, and the macroscopic inspections were carefully performed. After killing, the number of grossly visible tumors in the tongue, esophagus and other tissues were recorded, photos were taken and then the organs with lesions were processed for histopathological examination after fixation in 10% buffered formalin. Each tongue was cut in half longitudinally: one half was used for histopathology and immunohistochemistry and the remainder for PGE_2 determination. Five serial sections (4 μm each) were made from the tissue specimens after embedding in paraffin. One section was used for histopathology and the others for immunohistochemistry of the EP receptors, EP_1 and EP_2, proliferative cell nuclear antigen (PCNA) and cyclin D1.

The histopathological diagnosis was done on the sections stained with hematoxylin and eosin. Epithelial lesions (dysplasia and neoplasia) in the tongue and esophagus were diagnosed according to the criteria described by Kramer *et al.* (49). The multiplicities of the tongue and esophageal lesions were determined, as described above. An immunohistochemical analysis of EP_1 and EP_2 was performed as described above. The intensity and localization of the immunoreactivity against the EP_1 and EP_2 primary antibodies were determined on the tongue sections containing SCC using a microscope (Olympus BX41, Olympus Optical Co., Ltd, Tokyo, Japan) and evaluated for the intensity of the immunoreactivity of EP_1 and EP_2 on a 0–4+ scale. The overall intensity of the staining reaction was scored with 0 indicating no immunoreactivity and no positive cells, 1+ weak immunoreactivity and <10% positive cells, 2+ mild immunoreactivity and 10–30% positive cells, 3+ moderate immunoreactivity and 31–60% positive cells and 4+ strong immunoreactivity and 61–100% positive cells. To assess the proliferative activity of the tongue SCC developed in groups 1 through 4, the PCNA-labeling index was quantified. The immunohistochemical detection of PCNA-positive nuclei was done using an

immunohistochemical analysis kit (Dako Japan). The labeling indices were calculated by counting the PCNA-positive nuclei in at least 100 cells at three different fields of tongue and esophagus from each mouse. Cyclin D1 immunohistochemistry was also performed for the evaluation of cell cycle activity of tongue SCCs. Briefly, 4 μm paraffin-embedded sections from tongue SCCs developed in groups 1 through 4 were deparaffinized with three changes of xylene and hydrated using a graded series of alcohol. Slides were incubated twice in 1 mM ethylenediaminetetraacetic acid (pH 8.0) at 121°C in an autoclave, 5 min each to effect antigen retrieval before staining, then exposed overnight to 1:100 diluted cyclin D1 mouse monoclonal antibody (Novocastra Laboratories, Newcastle upon Tyne, UK). Slides were then developed by the avidin–biotin–peroxidase complex methods. Cells were considered positive for cyclin D1 when definite nuclear staining was identified. The positive cell ratio (percentage) for cyclin D1 was determined by randomly observing 100 cancer cells under magnification ×400 (>25 fields) to score. Positive cell ratios were calculated as numbers per 100 cells.

For the determination of the PGE_2 content, the tongue tissue (~100 mg) without tumors was obtained from groups 1–6 after killing. The samples were then placed into microcentrifuge tubes containing 1 ml of sodium phosphate buffer (10 mmol/l, pH 7.4) and finely minced with scissors for 15 s. The samples were then incubated for 20 min at 37°C in a shaking water bath. Following the incubation period, the samples were centrifuged at 9000*g* for 30 s and the supernatants collected. The supernatants were flash frozen in liquid nitrogen and stored at −80°C for subsequent determination of PGE_2 content. The PGE_2 level was assayed using the PGE_2 ELISA kit (Cayman Chemical Co.) according to the manufacturer's instructions.

Statistical analysis

A statistical analysis of the incidence of lesions was performed using Fisher's exact probability test, and the other results expressed as the mean ± SD were analyzed by Student–Newman–Keuls multiple comparison test using the GraphPad InStat software (version 3.05, GraphPad Software, San Diego, CA). A level of $P < 0.05$ was considered to be statistically significant.

Results

Animal model study

General observation. All Tg and non-Tg mice in groups 1–5 showed a good tolerance for 4-NQO-exposure in their drinking water. The growth curves during the study did not significantly differ among the groups with different treatment periods and between the two phenotypes (data not shown). After killing, the mean body, liver and relative liver weights did not significantly differ among the groups (data not shown).

Tongue and esophageal tumors development. Whereas no tumors or dysplastic lesions developed in any organs, including the tongue, esophagus and forestomach, of the non-Tg mice that received drinking water with or without 4-NQO, exophytic tongue and esophageal tumors developed in the Tg mice that received 4-NQO (Figure 1A). One large forestomach tumor, histologically diagnosed as an SCC, developed in a *ras*H2 mouse that received 4-NQO for 6 weeks. Such neoplasms were not observed in the untreated Tg mice. A large forestomach tumor developed in one mouse of group 3, but no tumors were observed in tissues other than the tongue and esophagus of any animals. The cumulative distribution of the tongue and tumors is illustrated in Figure 1B. When compared with the *ras*H2 mice that received 4-NQO for 2, 4 or 6 weeks, a number of tongue and esophageal tumors developed, distributed in whole parts of the tissues. The tongue and esophageal tumors were histopathologically PAP and SCC (Figure 1C). As summarized in Figure 2A, the number of tumors increased with the increased duration of 4-NQO-exposure: the highest incidence and multiplicity of tongue (100% incidence with a multiplicity of 2.80 ± 1.30 per tongue) and esophageal (60% incidence with a multiplicity of 1.40 ± 1.67 per esophagus) tumors were observed in the Tg mice given 4-NQO for 8 weeks. Preneoplastic lesions that were diagnosed to be dysplasia with various degrees of atypia also developed in the tongue and esophagus with or without tumors in the Tg mice that received 4-NQO (Figure 2B). The incidence and multiplicity of dysplasia were increased when the duration of the 4-NQO exposure was increased. In addition, the histopathological grade of dysplasia depended on the duration of the 4-NQO exposure.

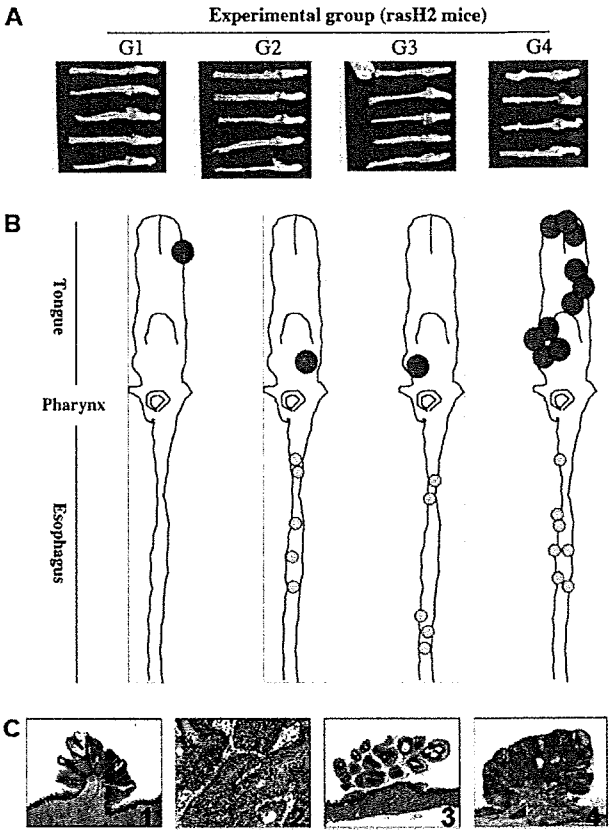

Fig. 1. Tongue and esophageal tumors developed in *ras*H2 mice that received 4-NQO in drinking water for 2 (G1, group 1), 4 (G2, group 2), 6 (G3, group 3) or 8 weeks (G4, group 4). (**A**) Macroscopic view of tongue and esophageal tumors. A large forestomach tumor developed in a *ras*H2 mouse of group 3. (**B**) Tumor distribution in the tongue and esophagus. (**C**) Histopathology of tongue and esophageal tumors: 1, tongue PAP; 2, tongue SCC; 3, esophageal PAP and 4, esophageal SCC. Hematoxylin and eosin stain, original magnification: 1, ×10; 2, ×50; 3, ×20 and 4, ×20.

EP receptors' immunohistochemistry of tongue and esophageal lesions. As indicated in Figure 3, the neoplasms and dysplasias that developed in the tongue and esophagus expressed EP_{1-4} receptors, while the expression in the non-lesional and normal squamous epithelium of the tongue and esophagus was quite low or absent. Among the EP receptors, EP_1 and EP_2 expressed as strongly positive in the dysplastic lesions and neoplasms in these tissues. The expression was observed in the cytoplasm of the cells that composed the lesions.

Chemoprevention study

General observation. All Tg mice belonging to groups 1–5 showed a good tolerance of the treatment with 4-NQO and/or pitavastatin. The mean body weight (29.0 ± 5.5 g) of group 2 (4-NQO → 1 p.p.m. pitavastatin) and the mean body (28.4 ± 4.5 g), liver (1.39 ± 0.23 g) and relative liver weights (4.89 ± 0.23 g/100 g body wt) of group 3 (4-NQO → 5 p.p.m. pitavastatin) were significantly lower than that (body weight, 35.9 ± 6.1 g; liver weight, 1.81 ± 0.29 g and relative liver weight, 5.07 ± 0.31 g/100 g body wt) of group 1 (4-NQO alone) at week 24 ($P < 0.05$, for each comparison). However, the values of group 4 (4-NQO→10 p.p.m. pitavastatin) were comparable with those of group 1 (data not shown).

Tongue and esophageal tumor development. As summarized in Table I, tongue tumors with a 100% incidence and a multiplicity of 2.20 ± 1.23 developed in *ras*H2 mice that received 4-NQO alone

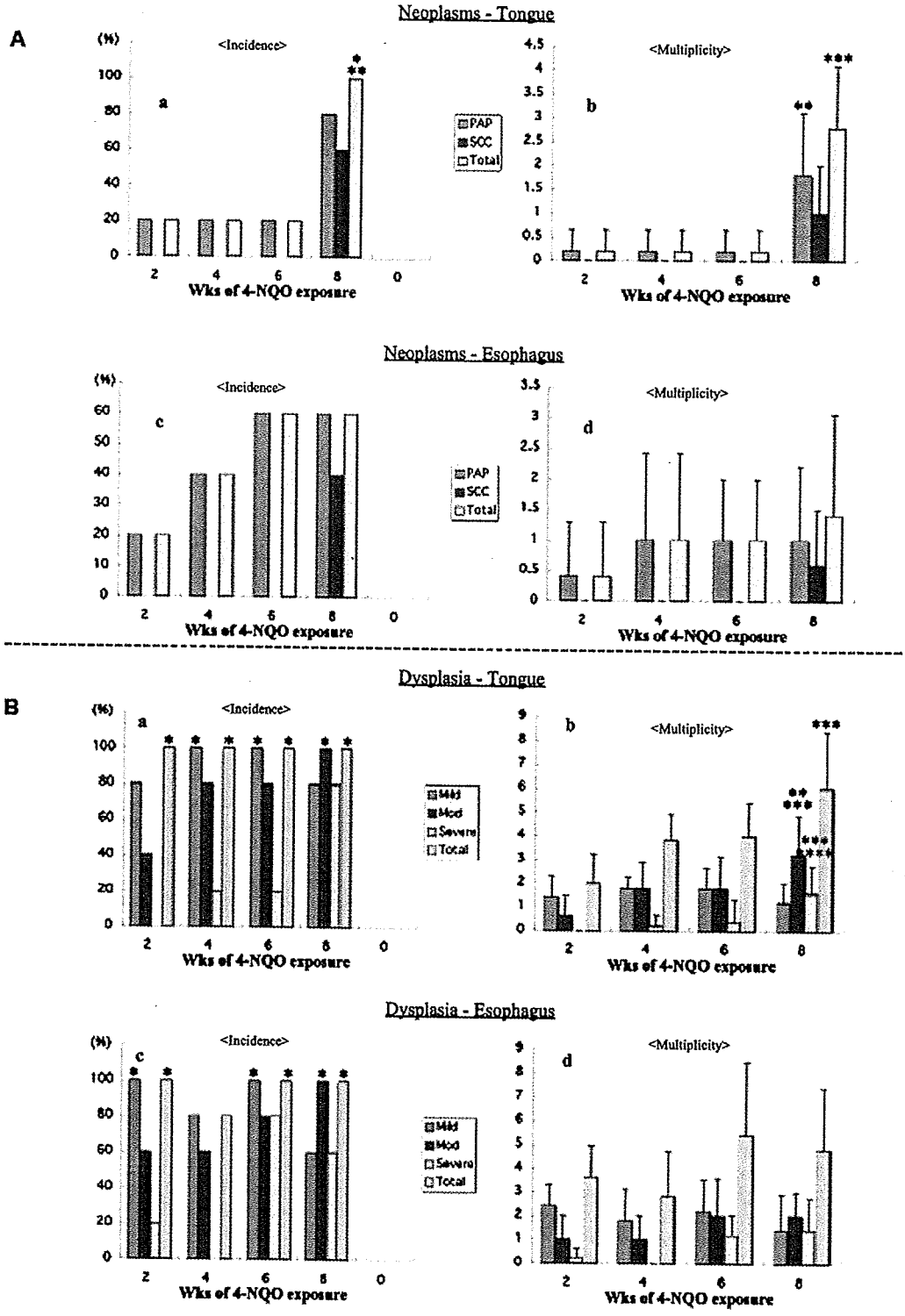

Fig. 2. Incidence and multiplicity of (A) tumors and (B) dysplasia that developed in the tongue and esophagus of *ras*H2 mice that received 4-NQO in their drinking water.

(group 1). Feeding with pitavastatin reduced the incidence and multiplicity of tongue tumors: 5 p.p.m. pitavastatin in the diet after 4-NQO-exposure significantly lowered the incidence and multiplicity of tongue PAP ($P = 0.03316$ and $P < 0.05$, respectively) and 10 p.p.m. pitavastatin in the diet significantly lowered the incidence of tongue PAP ($P = 0.0316$), SCC ($P = 0.0229$), total tumors (PAP + SCC, $P = 0.0065$) and the multiplicity of total tongue tumors ($P < 0.05$). Regarding tongue dysplasia, feeding with 1 and 5 p.p.m. pitavastatin significantly reduced the incidence of mild dysplasia ($P = 0.0065$ and $P = 0.0015$, respectively), and 10 p.p.m. pitavastatin in the diet

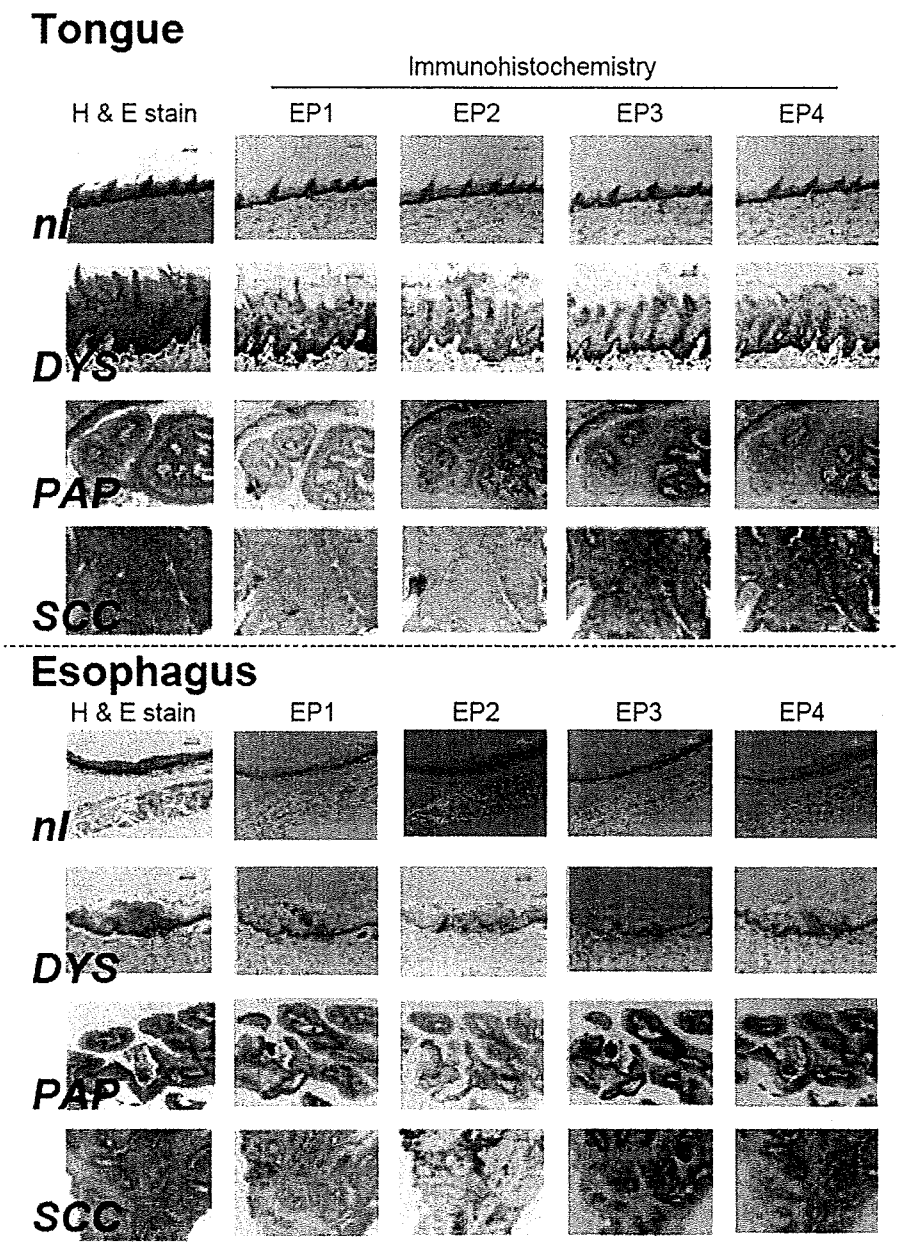

Fig. 3. Immunohistochemical expression of EP_{1-4} receptors in the normal epithelium and lesions induced by 4-NQO in tongue and esophagus. Expression of EP_{1-4} receptors is weak in the normal squamous epithelium of both tissues. Expression of EP_1 and EP_2 is strong in the dysplasia, PAP and SCC, whereas that of EP_3 and EP_4 is weak in the lesions. nl, normal squamous epithelium; DYS, squamous cell dysplasia. Hematoxylin and eosin stain and immunohistochemistry of EP_{1-4}, original magnification ×20.

significantly lowered the incidence of severe tongue dysplasia ($P = 0.0306$, Table I). Similarly, dietary feeding with 5 p.p.m. pitavastatin significantly reduced the multiplicity of mild dysplasia of the tongue ($P < 0.05$), and pitavastatin feeding at all dose levels significantly lowered the multiplicity of total dysplasia (mild, moderate and severe dysplasia) ($P < 0.01$ at 1 p.p.m., $P < 0.001$ at 5 and 10 p.p.m.).

Regarding esophageal tumors, the incidence of SCC was significantly reduced by feeding with 10 p.p.m. pitavastatin ($P = 0.0076$). Although the incidence and multiplicity of esophageal SCC and total tumors (PAP + SCC, Table II) decreased after the administration of pitavastatin at all dose levels, the reduction did not reach statistical significance (Table II). Treatment with pitavastatin at all dose levels lowered the multiplicity of esophageal dysplasia to various degrees; the differences were not significant (Table II).

PCNA-labeling index and cyclin D1-positive index of tongue SCC. The PCNA-labeling indexes of SCCs developed in the Tg mice belonging to groups 1–4 are illustrated in Figure 4. The index of group 1 (Figure 4A) was the greatest and that of group 4 (Figure 4A) was the lowest among the groups: group 1, 74.2 ± 9.9; group 2, 53.6 ± 15.0; group 3, 39.8 ± 7.7 and group 4, 33.4 ± 8 (Figure 4A). The values of groups 2 ($P < 0.01$), 3 ($P < 0.001$) and 4 ($P < 0.001$) were significantly smaller than those of group 1. The index of group 4 ($P < 0.01$) was also significantly lower than that of group 2. As to

Table I. Incidence and multiplicity of tongue dysplasia and neoplasms in the *ras*H2 mice that received 4-NQO and/or pitavastatin

Group no.	Treatment	Dysplasia								Tumor					
		Incidence				Multiplicity				Incidence			Multiplicity		
		Mild DYS[a]	Moderate DYS	Severe DYS	Total	Mild DYS	Moderate DYS	Severe DYS	Total	PAP	SCC	Total	PAP	SCC	Total
1	4-NQO alone	10/10 (100%)	10/10 (100%)	8/10 (100%)	10/10 (100%)	1.10 ± 0.32[b]	1.50 ± 0.71	1.40 ± 1.08	4.00 ± 1.41	9/10 (90%)	7/10 (70%)	10/10 (100%)	1.40 ± 0.84	0.80 ± 0.63	2.20 ± 1.23
2	4-NQO → 1 p.p.m. pitavastatin	3/8 (38%)c	5/8 (63%)	4/8 (50%)	8/8 (100%)	0.50 ± 0.76	0.75 ± 0.71	0.88 ± 1.13	2.00 ± 0.76d	4/8 (50%)	4/8 (50%)	6/8 (75%)	0.63 ± 0.74	0.50 ± 0.54	1.13 ± 0.99
3	4-NQO → 5 p.p.m. pitavastatin	2/8 (25%)e	7/8 (88%)	4/8 (50%)	8/8 (100%)	0.25 ± 0.46f	1.00 ± 0.54	0.63 ± 0.74	1.88 ± 0.64g	3/8 (38%)h	5/8 (63%)	7/8 (88%)	0.38 ± 0.52f	0.63 ± 0.52	1.00 ± 0.53
4	4-NQO → 10 p.p.m. pitavastatin	4/8 (50%)	5/8 (63%)	2/8 (25%)i	7/8 (88%)	0.50 ± 0.53	0.88 ± 0.84	0.38 ± 0.74	1.75 ± 1.04g	3/8 (38%)h	1/8 (13%)j	3/8 (38%)c	0.63 ± 0.92	0.13 ± 0.35	0.75 ± 1.04f
5	10 p.p.m. pitavastatin	0/4 (0%)	0/4 (0%)	0/4 (0%)	0/4 (0%)	0	0	0	0	0/4 (0%)	0/4 (0%)	0/4 (0%)	0	0	0
6	None	0/4 (0%)	0/4 (0%)	0/4 (0%)	0/4 (0%)	0	0	0	0	0/4 (0%)	0/4 (0%)	0/4 (0%)	0	0	0

[a]DYS, squamous cell dysplasia.
[b]Mean ± SD.
Significantly different from group 1 based on the Fisher's exact probability test ([c] $P = 0.0065$, [e] $P = 0.0015$, [h] $P = 0.0316$, [i] $P = 0.0306$ and [j] $P = 0.0229$).
Significantly different from group 1 based on the Tukey–Kramer multiple comparison test ([d] $P < 0.01$, [f] $P < 0.05$ and [g] $P < 0.001$).

Table II. Incidence and multiplicity of esophageal dysplasia and neoplasms in the *ras*H2 mice that received 4-NQO and/or pitavastatin

Group no.	Treatment	Dysplasia								Tumor					
		Incidence				Multiplicity				Incidence			Multiplicity		
		Mild DYS[a]	Moderate DYS	Severe DYS	Total	Mild DYS	Moderate DYS	Severe DYS	Total	PAP	SCC	Total	PAP	SCC	Total
1	4-NQO alone	9/10 (90%)	10/10 (100%)	7/10 (70%)	10/10 (100%)	1.50 ± 0.71[b]	2.60 ± 1.17	1.40 ± 1.27	5.50 ± 2.37	5/10 (50%)	8/10 (80%)	9/10 (90%)	1.00 ± 1.25	1.40 ± 1.17	2.40 ± 1.96
2	4-NQO → 1 p.p.m. pitavastatin	6/8 (75%)	8/8 (100%)	6/8 (75%)	8/8 (100%)	0.25 ± 1.04	2.38 ± 1.06	1.13 ± 0.99	4.75 ± 1.98	3/8 (38%)	5/8 (63%)	6/8 (75%)	0.50 ± 0.76	1.00 ± 0.93	1.50 ± 1.31
3	4-NQO → 5 p.p.m. pitavastatin	5/8 (63%)	8/8 (100%)	6/8 (75%)	8/8 (100%)	1.00 ± 0.93	2.63 ± 0.74	1.50 ± 1.31	5.13 ± 1.55	4/8 (50%)	4/8 (50%)	5/8 (63%)	0.88 ± 0.99	0.63 ± 0.74	1.50 ± 1.41
4	4-NQO → 10 p.p.m. pitavastatin	6/8 (75%)	7/8 (88%)	6/8 (75%)	8/8 (100%)	1.00 ± 0.93	1.63 ± 1.19	1.13 ± 0.84	3.75 ± 2.32	5/8 (63%)	1/8 (13%)[c]	5/8 (63%)	1.16 ± 1.13	0.25 ± 0.71	1.38 ± 1.51
5	10 p.p.m. pitavastatin	0/4 (0%)	0/4 (0%)	0/4 (0%)	0/4 (0%)	0	0	0	0	0/4 (0%)	0/4 (0%)	0/4 (0%)	0	0	0
6	None	0/4 (0%)	0/4 (0%)	0/4 (0%)	0/4 (0%)	0	0	0	0	0/4 (0%)	0/4 (0%)	0/4 (0%)	0	0	0

[a]DYS, squamous cell dysplasia.
[b]Mean ± SD.
[c]Significantly different from group 1 based on the Fisher's exact probability test ($P = 0.0076$).

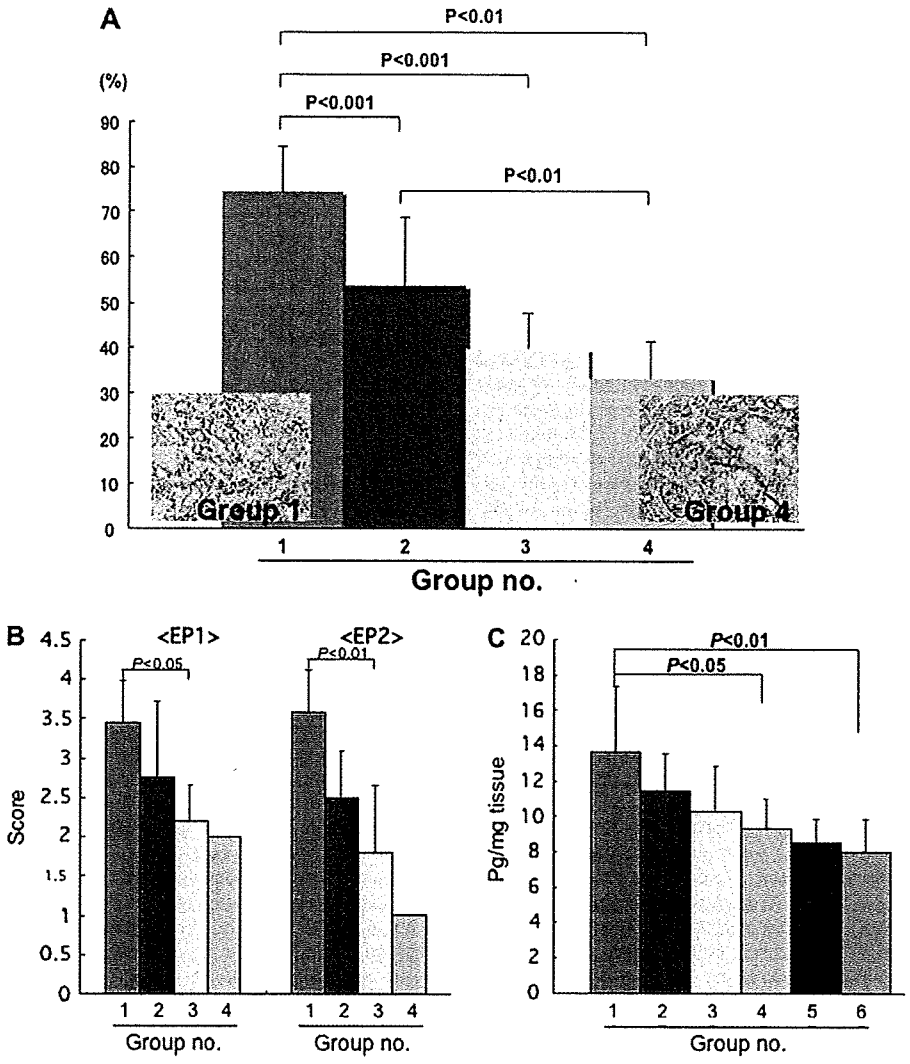

Fig. 4. Immunohistochemical analysis of PCNA-labeling index and EP_1/EP_2 expression of tongue SCCs and PGE_2 levels of the tongue (preclinical chemoprevention study). (A) PCNA-labeling indices (mean ± SD) of tongue SCCs in groups 1–4. Inserts are PCNA-immunohistochemistry from a SCC developed in group 1 that received 4-NQO alone (original magnification, ×50) and in group 4 that received 4-NQO and 10 p.p.m. pitavastatin (original magnification, ×50). (B) Scores of immunohistochemical expression of EP_1 and EP_2 receptors in tongue SCCs developed in groups 1–4. (C) PGE_2 contents in the tongue without tumors.

cyclin D1-positive index (mean ± SD or mean) of SCCs, the values of groups 2 ($n = 5$, 38.00 ± 6.28, $P < 0.01$), 3 ($n = 4$, 24.50 ± 9.26, $P < 0.001$) and 4 ($n = 1$, 24.50) were smaller than that of group 1 (57.00 ± 8.21, $n = 8$).

Scores of EP_1 and EP_2 receptors' immunoreactivities in the tongue SCC. As shown in Figure 4B, the tongue SCC that developed in groups 1–4 expressed EP_1 and EP_4 receptors, the strongest being the SCC of group 1. The dietary pitavastatin reduced the score of both EP_1 and EP_2 reactivity, and the values of group 3 were significantly lower than those of group 1 (EP_1 for $P < 0.05$ and EP_2 for $P < 0.01$). The mean values (2 for EP_1 and 1 for EP_2) of group 4 were also low, but a statistical analysis could not be done because of the small sample size from group 4.

Tongue PGE_2 level. The PGE_2 content of the tongue is illustrated in Figure 4C. The PGE_2 content (13.60 ± 3.66 pg/mg tissue, $P < 0.01$) of group 1 (4-NQO alone) was significantly greater than group 6 (untreated, 8.00 ± 1.83 pg/mg tissue). The pitavastatin feeding reduced the level and the value of group 4 (4-NQO → 10 p.p.m. pitavastatin, 9.25 ± 1.67 pg/mg tissue) was significantly smaller than that of group 1 ($P < 0.05$). The value of group 5 (10 p.p.m. pitavastatin, 8.50 ± 1.29 pg/mg tissue) was comparable with that (8.00 ± 1.80) seen in group 6.

Discussion

In this study, we demonstrated that *ras*H2 mice are highly susceptible to a genotoxic carcinogen, 4-NQO, in drinking water and many neoplasms developed in their tongue and esophagus within the 24 experimental weeks. Interestingly, the EP receptors, especially EP1 and EP2, were immunohistochemically expressed in the lesions (dysplasia and neoplasm) induced by 4-NQO in these tissue specimens. This novel animal carcinogenesis model is useful to investigate field cancerization in the head and neck regions (oral cavity and esophagus) (6,7). The model also can be used to identify cancer chemopreventive agents in these tissues, as we revealed that dietary pitavastatin was

capable of inhibiting the tumor development in the tissue specimens, especially the tongue.

Similar to the high frequency of *p53* mutation in human oral cancers (50), a high percentage of *ras* mutation is also detected in Indian patients (51), but infrequently in white Caucasian populations (52). Especially, a high frequency of mutation in codons 12 and 61 of the H-*ras* gene was observed in chewing tobacco-related oral cancers in India (20). Among the *ras* genes, mutations of the H-*ras* (28%) and K-*ras* genes (33%), but not the N-*ras* gene, were found in oral tumors from the eastern Indian population (51). Therefore, the *ras* gene mutation is relatively high in oral cancer associated with tobacco chewing, and *ras* and *p53* mutational events might be independent and mutually exclusive (53).

Our previous work (24) demonstrated that c-Ha-*ras* proto-oncogene transgenic rats are highly susceptible to 4-NQO-induced carcinogensis in the tongue, but not the esophagus. Other different findings from the c-Ha-*ras* proto-oncogene transgenic rats are that the tongue tumors distributed throughout the dorsal site of the tongue in this study, whereas the tongue tumors developed in the dorsal site of the root of the tongue of the c-Ha-*ras* proto-oncogene transgenic rats that received 4-NQO in their drinking water (24). The reasons for this are not known, but the species difference and/or the difference in the distribution of an enzyme (DT-diaphorase) that catalyzes the conversion of 4-NQO to an ultimate carcinogen, 4-hydroxyaminoquinoline 1-oxide (54), in the tongue may reflect the differences observed.

In the current study, tongue and esophageal tumors developed in the *ras*H2 mice that received 4-NQO (20 p.p.m. in drinking water) for 4–8 weeks. Similar findings have been reported by Tang *et al.* (18), who were able to induce numerous tumors in these tissues of CBA and C57BL/6 mice when given 4-NQO in drinking water for 16 weeks. Their extensive work also indicated alterations in the expression of intermediate filaments (K14 and K1), proliferation activity by estimating bromodeoxyuridine-positive nuclei and a cell cycle inhibitor, p16. In this study, we observed that 4-NQO-induced tongue and esophageal carcinogenesis depends on the duration of a carcinogen treatment and that 4 weeks of treatment is sufficient to induce tumors in two tissues. As Tang *et al.* (18) did not observe any tumors in the tissue specimens other than the tongue and esophagus, we found only one forestomach tumor in a *ras*H2 mouse that received 4-NQO for 6 weeks. In our previous investigation using c-Ha-*ras* proto-oncogene transgenic rats, no tumors developed in their forestomach when given 4-NQO in drinking water. Recently, Fong *et al.* (55) have reported interesting findings that rats given 4-NQO in drinking water and fed a zinc-deficient diet developed tumors in the tongue, esophagus and forestomach, whereas those given 4-NQO and a zinc-sufficient diet had tumors occur only in the tongue, suggesting that dietary modulation, including zinc, influences a manifestation of field cancerization.

Regarding mice genetically modified for tongue carcinogenesis, the *p53* transgenic mice have been reported to be highly susceptible to 4-NQO-induced oral cancer (56). When the palate of the $p53^{Val135/WT}$ mice was treated by the direct application of 4-NQO with a hairbrush, which had been dipped in 4-NQO solution, thrice weekly for 16 weeks and followed by no further treatment for 32 weeks, a greater incidence and multiplicity of squamous cell tumors in the oral cavity, esophagus and forestomach were observed in comparison with the $p53^{WT/WT}$ mice at 48 experimental weeks. Their microarray data suggest the importance of the *p53* mutation, alteration in *p53*-dependent apoptosis and cell proliferation during the carcinogenesis of these tissues. These findings also supported the belief that the crosstalk of apoptosis, cell cycle arrest, transforming growth factor β signaling pathway and *Ras*-mitogen-activated protein kinase pathway may be involved in tumorigenesis. In the current study, we observed numerous tumors mainly in the tongue and esophagus, occurring as early as 24 weeks, although no *p53* mutations were determined. Recently, Caulin *et al.* (57) developed an interesting mouse model without the use of a carcinogen, in which the focal activation of an oncogenic K-*rasG12D* allele in the oral squamous epithelium resulted in the development of a number of oral cavity tumors with an altered expression pattern of keratin 16 weeks after the activation. Taken together, *ras* mutation and/or activation as well as *p53* mutation are therefore considered to be involved in oral cancer development.

Using *ras*H2 mice, we investigated the chemopreventive ability of pitavastatin in 4-NQO-induced tongue and esophageal carcinogenesis. The dietary pitavastatin is therefore considered to have the potential to suppress the development of tongue tumorigenesis, whereas the potential in esophageal carcinogenesis was relatively weak in comparison with that observed in tongue carcinogenesis. The reasons for this are not known, but a different bioavailability of dietary pitavastatin in these tissues is considered to be one possible explanation. In this study, the PGE_2 content in the tongue was lowered by the treatment with pitavastatin. The findings support our previous results that lowering the PGE_2 content by treatment with COX-2 inhibitors (24,32) and a non-steroidal anti-inflammatory drug (58) suppresses 4-NQO-induced carcinogenesis. In this study, the dietary administration of pitavastatin reduced the immunohistochemical expression of EP_1 and EP_2 in the tongue, thus suggesting the involvement of these receptors in tongue carcinogenesis. The inhibitory effects of pitavastatin on carcinogenesis has recently been observed in colon tumorigenesis in our laboratory (43). In addition, an EP_2 antagonist, ONO-8711, in the diet effectively inhibits tongue tumor development in human c-Ha-*ras* transgenic rats initiated with 4-NQO (41). Besides these effects of pitavastatin, we observed that dietary pitavastatin at all doses significantly lowers the PCNA-labeling index of tongue SCCs, thus suggesting that this drug is able to inhibit the growth of tongue SCCs possibly through affecting events during the tumor progression stage. Additionally, feeding with pitavastatin (groups 2–4) reduced the cyclin D1-positive rates of cancer cells when compared with group 1 (4-NQO alone). The findings are of interest, because H-*ras* and cyclin D1, a downstream of the *Ras*, influence the susceptibility of oral cancer (21). Thus, the multiple effects of pitavastatin on the expression of EP_1 and EP_2 receptors, PGE_2 content, proliferation and cell cycle may result in inhibition of tongue carcinogenesis initiated with 4-NQO in *ras*H2 mice.

Using this model, detailed research on molecular and proteomics events, such as the involvement of inflammation in tongue/esophageal carcinogenesis, could be conducted to fight oral and esophageal epithelial malignancies. In addition, the gene–environment and gene–gene interactions in the carcinogenesis (59) of these tissues can be investigated using this *ras*H2 mouse model, since the H-*ras* gene and other members of the *ras* gene family also appear to be a common target for the coding sequence mutations in the initiation of carcinogenesis at several organ sites and in various species by specific carcinogens (60).

Funding

The Ministry of Health, Labour and Welfare of Japan; the Ministry of Education, Culture, Sports, Science and Technology of Japan (18592076 and 17015016); the High-Technology Center of Kanazawa Medical University (H2007-12).

Acknowledgements

Conflict of Interest Statement: None declared.

References

1. Parkin,D.M. *et al.* (2005) Global cancer statistics, 2002. *CA Cancer J. Clin.*, **55**, 74–108.
2. Llewellyn,C.D. *et al.* (2004) An analysis of risk factors for oral cancer in young people: a case-control study. *Oral Oncol.*, **40**, 304–313.
3. Mackenzie,J. *et al.* (2000) Increasing incidence of oral cancer amongst young persons: what is the aetiology? *Oral Oncol.*, **36**, 387–389.
4. Scully,C. *et al.* (2000) ABC of oral health. Oral cancer. *BMJ*, **321**, 97–100.
5. Kanojia,D. *et al.* (2006) 4-Nitroquinoline-1-oxide induced experimental oral carcinogenesis. *Oral Oncol.*, **42**, 655–667.

6. Braakhuis,B.J. *et al.* (2003) A genetic explanation of Slaughter's concept of field cancerization: evidence and clinical implications. *Cancer Res.*, **63**, 1727–1730.
7. Ha,P.K. *et al.* (2003) The molecular biology of mucosal field cancerization of the head and neck. *Crit. Rev. Oral Biol. Med.*, **14**, 363–369.
8. van Oijen,M.G. *et al.* (2000) Oral field cancerization: carcinogen-induced independent events or micrometastatic deposits? *Cancer Epidemiol. Biomarkers Prev.*, **9**, 249–256.
9. Brown,K.S. *et al.* (2006) Chemoprevention of squamous cell carcinoma of the oral cavity. *Otolaryngol. Clin. North Am.*, **39**, 349–363.
10. Tanaka,T. (1995) Chemoprevention of oral carcinogenesis. *Eur. J. Cancer B Oral Oncol.*, **31B**, 3–15.
11. Nagao,T. *et al.* (2005) Incidence rates for oral leukoplakia and lichen planus in a Japanese population. *J. Oral Pathol. Med.*, **34**, 532–539.
12. Ha,P.K. *et al.* (2006) Promoter methylation and inactivation of tumour-suppressor genes in oral squamous-cell carcinoma. *Lancet Oncol.*, **7**, 77–82.
13. Lo Muzio,L. (2001) A possible role for the WNT-1 pathway in oral carcinogenesis. *Crit. Rev. Oral Biol. Med.*, **12**, 152–165.
14. Schwartz,J.L. (2000) Biomarkers and molecular epidemiology and chemoprevention of oral carcinogenesis. *Crit. Rev. Oral Biol. Med.*, **11**, 92–122.
15. Sotiriou,C. *et al.* (2004) Molecular profiling of head and neck tumors. *Curr. Opin. Oncol.*, **16**, 211–214.
16. Mognetti,B. *et al.* (2006) Animal models in oral cancer research. *Oral Oncol.*, **42**, 448–460.
17. Tanaka,T. *et al.* (1991) Alterations of the nucleolar organizer regions during 4-nitroquinoline 1-oxide-induced tongue carcinogenesis in rats. *Carcinogenesis*, **12**, 329–333.
18. Tang,X.H. *et al.* (2004) Oral cavity and esophageal carcinogenesis modeled in carcinogen-treated mice. *Clin. Cancer Res.*, **10**, 301–313.
19. Vered,M. *et al.* (2005) 4NQO oral carcinogenesis: animal models, molecular markers and future expectations. *Oral Oncol.*, **41**, 337–339.
20. Saranath,D. *et al.* (1991) High frequency mutation in codons 12 and 61 of H-*ras* oncogene in chewing tobacco-related human oral carcinoma in India. *Br. J. Cancer*, **63**, 573–578.
21. Sathyan,K.M. *et al.* (2006) Influence of single nucleotide polymorphisms in H-*Ras* and cyclin D1 genes on oral cancer susceptibility. *Oral Oncol.*, **42**, 607–613.
22. Vairaktaris,E. *et al.* (2007) Expression of ets-1 is not affected by N-*ras* or H-*ras* during oral oncogenesis. *J. Cancer Res. Clin. Oncol.*, **133**, 227–233.
23. Rumsby,G. *et al.* (1990) Low incidence of ras oncogene activation in human squamous cell carcinomas. *Br. J. Cancer*, **61**, 365–368.
24. Suzuki,R. *et al.* (2006) An animal model for the rapid induction of tongue neoplasms in human c-Ha-*ras* proto-oncogene transgenic rats by 4-nitroquinoline 1-oxide: its potential use for preclinical chemoprevention studies. *Carcinogenesis*, **27**, 619–630.
25. Saitoh,A. *et al.* (1990) Most tumors in transgenic mice with human c-Ha-ras gene contained somatically activated transgenes. *Oncogene*, **5**, 1195–1200.
26. Pritchard,J.B. *et al.* (2003) The role of transgenic mouse models in carcinogen identification. *Environ. Health Perspect.*, **111**, 444–454.
27. Tamaoki,N. (2001) The rasH2 transgenic mouse: nature of the model and mechanistic studies on tumorigenesis. *Toxicol. Pathol.*, **29** (suppl.), 81–89.
28. Maruyama,C. *et al.* (2001) Overexpression of human H-*ras* transgene is responsible for tumors induced by chemical carcinogens in mice. *Oncol. Rep.*, **8**, 233–237.
29. Yanaida,Y. *et al.* (2002) Dietary silymarin suppresses 4-nitroquinoline 1-oxide-induced tongue carcinogenesis in male F344 rats. *Carcinogenesis*, **23**, 787–794.
30. Smith,W.L. *et al.* (2000) Cyclooxygenases: structural, cellular, and molecular biology. *Annu. Rev. Biochem.*, **69**, 145–182.
31. Bertagnolli,M.M. (2007) Cox-2 and cancer chemoprevention: picking up the pieces. *Recent Results Cancer Res.*, **174**, 73–78.
32. Yoshida,K. *et al.* (2003) A COX-2 inhibitor, nimesulide, inhibits chemically-induced rat tongue carcinogenesis through suppression of cell proliferation activity and COX-2 and iNOS expression. *Histol. Histopathol.*, **18**, 39–48.
33. Sawhney,M. *et al.* (2007) Expression of NF-kappaB parallels COX-2 expression in oral precancer and cancer: association with smokeless tobacco. *Int. J. Cancer*, **120**, 2545–2556.
34. Vishwanatha,J.K. *et al.* (2003) Modulation of annexin I and cyclooxygenase-2 in smokeless tobacco-induced inflammation and oral cancer. *Mol. Cell Biochem.*, **248**, 67–75.
35. Kitamura,T. *et al.* (2003) Combined effects of prostaglandin E receptor subtype EP_1 and EP_4 antagonists on intestinal tumorigenesis in adenomatous poliposis coli gene knockout mice. *Cancer Sci.*, **94**, 618–621.
36. Kitamura,T. *et al.* (2002) Inhibitory effects of mofezolac, a cyclooxygenase-1 selective inhibitor, on intestinal carcinogenesis. *Carcinogenesis*, **23**, 1463–1466.
37. Mutoh,M. *et al.* (2006) Roles of prostanoids in colon carcinogenesis and their potential targeting for cancer chemoprevention. *Curr. Pharm. Des.*, **12**, 2375–2382.
38. Narumiya,S. *et al.* (2001) Genetic and pharmacological analysis of prostanoid receptor function. *J. Clin. Invest.*, **108**, 25–30.
39. Lee,J.L. *et al.* (2005) Differential expression of E prostanoid receptors in murine and human non-melanoma skin cancer. *J. Invest. Dermatol.*, **125**, 818–825.
40. Chun,K.S. *et al.* (2007) Cyclooxygenase-2 inhibits UVB-induced apoptosis in mouse skin by activating the prostaglandin E2 receptors, EP2 and EP4. *Cancer Res.*, **67**, 2015–2021.
41. Makita,H. *et al.* (2007) A prostaglandin E_2 receptor subtype EP_1-selective antagonist, ONO-8711, suppresses 4-nitroquinoline 1-oxide-induced rat tongue carcinogenesis. *Carcinogenesis*, **28**, 677–684.
42. Morton,D. *et al.* (2002) The Tg rasH2 mouse in cancer hazard identification. *Toxicol. Pathol.*, **30**, 139–146.
43. Yasui,Y. *et al.* (2007) A lipophilic statin, pitavastatin, suppresses inflammation-associated mouse colon carcinogenesis. *Int. J. Cancer.*, **121**, 2331–2339.
44. Sathyan,K.M. *et al.* (2007) H-*Ras* mutation modulates the expression of major cell cycle regulatory proteins and disease prognosis in oral carcinoma. *Mod. Pathol.*, **20**, 1141–1148.
45. Rao,K.N. (1995) The significance of the cholesterol biosynthetic pathway in cell growth and carcinogenesis (review). *Anticancer Res.*, **15**, 309–314.
46. Yu,H.Y. *et al.* (2005) Statin attenuates high glucose-induced and angiotensin II-induced MAP kinase activity through inhibition of NAD(P)H oxidase activity in cultured mesangial cells. *Med. Chem.*, **1**, 461–466.
47. Huang,Z. *et al.* (2007) Enhanced levels of glutathione and protein glutathiolation in rat tongue epithelium during 4-NQO-induced carcinogenesis. *Int. J. Cancer*, **120**, 1396–1401.
48. Inoue,I. *et al.* (2000) Lipophilic HMG-CoA reductase inhibitor has an anti-inflammatory effect: reduction of MRNA levels for interleukin-1beta, interleukin-6, cyclooxygenase-2, and p22phox by regulation of peroxisome proliferator-activated receptor alpha (PPARalpha) in primary endothelial cells. *Life Sci.*, **67**, 863–876.
49. Kramer,I.R. *et al.* (1978) Definition of leukoplakia and related lesions: an aid to studies on oral precancer. *Oral Surg. Oral Med. Oral Pathol.*, **46**, 518–539.
50. Brinkman,B.M. *et al.* (2006) Disease mechanism and biomarkers of oral squamous cell carcinoma. *Curr. Opin. Oncol.*, **18**, 228–233.
51. Das,N. *et al.* (2000) Ras gene mutations in oral cancer in eastern India. *Oral Oncol.*, **36**, 76–80.
52. Warnakulasuriya,K.A. *et al.* (1992) Point mutations in the Ha-*ras* oncogene are detectable in formalin-fixed tissues of oral squamous cell carcinomas, but are infrequent in British cases. *J. Oral. Pathol. Med.*, **21**, 225–229.
53. Munirajan,A.K. *et al.* (1998) Detection of a rare point mutation at codon 59 and relatively high incidence of H-*ras* mutation in Indian oral cancer. *Int. J. Oncol.*, **13**, 971–974.
54. Sugimura,T. *et al.* (1966) The metabolism of 4-nitroquinoline-1-oxide, a carcinogen. 3. An enzyme catalyzing the conversion of 4-nitroquinoline-1-oxide to 4-hydroxyaminoquinoline-1-oxide in rat liver and hepatomas. *Cancer Res.*, **26**, 1717–1721.
55. Fong,L.Y. *et al.* (2005) Dietary zinc modulation of COX-2 expression and lingual and esophageal carcinogenesis in rats. *J. Natl Cancer Inst.*, **97**, 40–50.
56. Zhang,Z. *et al.* (2006) p53 transgenic mice are highly susceptible to 4-nitroquinoline-1-oxide-induced oral cancer. *Mol. Cancer Res.*, **4**, 401–410.
57. Caulin,C. *et al.* (2004) Inducible activation of oncogenic K-*ras* results in tumor formation in the oral cavity. *Cancer Res.*, **64**, 5054–5058.
58. Tanaka,T. *et al.* (1989) Inhibitory effects of non-steroidal anti-inflammatory drugs, piroxicam and indomethacin on 4-nitroquinoline 1-oxide-induced tongue carcinogenesis in male ACI/N rats. *Cancer Lett.*, **48**, 177–182.
59. Shields,P.G. *et al.* (2000) Cancer risk and low-penetrance susceptibility genes in gene-environment interactions. *J. Clin. Oncol.*, **18**, 2309–2315.
60. Yuspa,S.H. *et al.* (1988) Chemical carcinogenesis: from animal models to molecular models in one decade. *Adv. Cancer Res.*, **50**, 25–70.

Received August 1, 2007; revised September 27, 2007; accepted September 27, 2007

The EMBO Journal (2008) 27, 1671–1681 | © 2008 European Molecular Biology Organization | Some Rights Reserved 0261-4189/08
www.embojournal.org

THE EMBO JOURNAL

EMBO open

Activated macrophages promote Wnt signalling through tumour necrosis factor-α in gastric tumour cells

Keisuke Oguma[1,6], Hiroko Oshima[1,6], Masahiro Aoki[2], Ryusei Uchio[1], Kazuhito Naka[3], Satoshi Nakamura[4], Atsushi Hirao[3], Hideyuki Saya[5], Makoto Mark Taketo[2] and Masanobu Oshima[1,*]

[1]Division of Genetics, Cancer Research Institute, Kanazawa University, Kanazawa, Japan, [2]Department of Pharmacology, Kyoto University Graduate School of Medicine, Kyoto, Japan, [3]Division of Molecular Genetics, Cancer Research Institute, Kanazawa University, Kanazawa, Japan, [4]Department of Biomedical Research and Development, Link Genomics, Tokyo, Japan and [5]Division of Gene Regulation, Institute for Advanced Medical Research, Keio University School of Medicine, Tokyo, Japan

The activation of Wnt/β-catenin signalling has an important function in gastrointestinal tumorigenesis. It has been suggested that the promotion of Wnt/β-catenin activity beyond the threshold is important for carcinogenesis. We herein investigated the role of macrophages in the promotion of Wnt/β-catenin activity in gastric tumorigenesis. We found β-catenin nuclear accumulation in macrophage-infiltrated dysplastic mucosa of the *K19-Wnt1* mouse stomach. Moreover, macrophage depletion in $Apc^{\Delta 716}$ mice resulted in the suppression of intestinal tumorigenesis. These results suggested the role of macrophages in the activation of Wnt/β-catenin signalling, which thus leads to tumour development. Importantly, the conditioned medium of activated macrophages promoted Wnt/β-catenin signalling in gastric cancer cells, which was suppressed by the inhibition of tumour necrosis factor (TNF)-α. Furthermore, treatment with TNF-α induced glycogen synthase kinase 3β (GSK3β) phosphorylation, which resulted in the stabilization of β-catenin. We also found that *Helicobacter* infection in the *K19-Wnt1* mouse stomach caused mucosal macrophage infiltration and nuclear β-catenin accumulation. These results suggest that macrophage-derived TNF-α promotes Wnt/β-catenin signalling through inhibition of GSK3β, which may contribute to tumour development in the gastric mucosa.

The EMBO Journal (2008) **27**, 1671–1681. doi:10.1038/emboj.2008.105; Published online 29 May 2008
Subject Categories: signal transduction; molecular biology of disease

Keywords: gastric cancer; inflammation; macrophage; tumour necrosis factor-α; Wnt

Introduction

The canonical Wnt signalling pathway (Wnt/β-catenin pathway) operates by stabilizing β-catenin (Taketo, 2006). The phosphorylation of β-catenin by glycogen synthase kinase 3β (GSK3β) results in degradation through the ubiquitin pathway. The binding of Wnt ligands to a Frizzled receptor leads to inhibition of the β-catenin degradation complex consisting of APC, AXIN and GSK3β thereby allowing the nuclear translocation of stabilized β-catenin followed by transcriptional activation of the Wnt target genes. Wnt/β-catenin signalling has an important function in the maintenance of intestinal stem cells and progenitor cells (Korinek *et al*, 1998; van de Wetering *et al*, 2002), and its activation causes gastrointestinal tumour development (Oshima *et al*, 1995, 2006; Fodde *et al*, 2001).

The activation level of Wnt/β-catenin signalling has been reported to be a determining factor for the multiplicity of intestinal polyposis in several types of *Apc* gene mutant mice (Gaspar and Fodde, 2004; Li *et al*, 2005). Moreover, nuclear β-catenin accumulation is predominantly observed in the invasion front of colon cancer in comparison to the non-invasive tumour area (Brabletz *et al*, 1998). Furthermore, sensitivity of embryonic stem (ES) cells for differentiation is inhibited by increase of Wnt/β-catenin signalling activity (Kielman *et al*, 2002). These results, taken together, suggest that the promotion of the Wnt/β-catenin activity beyond the threshold level is required for tumorigenesis, invasion and the maintenance of cell stemness.

On the other hand, it has been established that inflammation has an important function in cancer development (Coussens and Werb, 2002). The activation of tumour necrosis factor (TNF)-α or NF-κB pathway is required for the development of hepatocellular carcinoma (Pikarsky *et al*, 2004) and intestinal tumours (Greten *et al*, 2004; Popivanova *et al*, 2008) through the induction of growth factors and suppression of apoptosis. Although several signalling pathways have been reported for the promotion of Wnt/β-catenin activity (Fodde and Brabletz, 2007), it has not been elucidated yet whether the inflammatory response contributes to the promotion of Wnt/β-catenin signalling during tumorigenesis.

Gastric cancer is the second most common cancer in the world and it is closely associated with *Helicobacter pylori* infection, which leads to chronic inflammation (Correa, 2003). Moreover, the activation of the Wnt/β-catenin

*Corresponding author. Division of Genetics, Cancer Research Institute, Kanazawa University, 13-1 Takara-machi, Kanazawa 920-0934, Japan. Tel.: +81 76 265 2721; Fax: +81 76 234 4519;
E-mail: oshimam@kenroku.kanazawa-u.ac.jp
[6]These authors contributed equally to this work

Received: 7 January 2008; accepted: 29 April 2008; published online: 29 May 2008

signalling is found in about 30% of gastric cancer (Clements *et al*, 2002), suggesting that Wnt activation is one of the major causes for gastric cancer development. We recently showed that cooperation of Wnt signalling and prostaglandin E_2 (PGE_2) pathway causes gastric cancer development in a transgenic mouse model (Oshima *et al*, 2006). Because the activation of PGE_2 signalling induces infiltration and activation of macrophages in the gastric mucosa (Oshima *et al*, 2004, 2005), these results collectively suggest that activated macrophages promote the Wnt/β-catenin signalling activity, which thus contributes to gastric cancer.

We herein show that TNF-α derived from activated macrophages promotes the Wnt/β-catenin activity in gastric cancer cells through the suppression of GSK3β. Moreover, *Helicobacter* infection in the *Wnt1* transgenic mice resulted in macrophage infiltration and the activation of Wnt/β-catenin signalling in the gastric mucosa, which thus led to gastric tumorigenesis. These results suggest that activated macrophages in inflammatory microenvironment have an important function in gastric tumorigenesis through the promotion of the Wnt/β-catenin activity.

Results

Macrophage infiltration and β-catenin nuclear accumulation in gastric dysplasia of K19-Wnt1 transgenic mice

K19-Wnt1 transgenic mice expressing *Wnt1* in the gastric epithelial cells develop sporadic dysplastic lesions in the glandular stomach (Oshima *et al*, 2006). In these dysplastic lesions, inflammatory cells infiltrated the submucosa, whereas cell infiltration was rarely detected in the adjacent normal mucosa (Figure 1A). By immunostaining, we found macrophage infiltration in the dysplastic mucosa, whereas tissue macrophages were only sparsely scattered in the normal mucosa (Figure 1B and H). We also found strong nuclear staining of β-catenin in the epithelial cells of the dysplastic mucosa (Figure 1C). Notably, β-catenin-accumulated epithelial cells were physically associated with stromal macrophages in the dysplastic lesions (Figure 1E). In contrast, mild β-catenin accumulation was found only in the cell proliferation zone of the normal mucosa (Figure 1I). We confirmed the increase in the β-catenin-positive index in the dysplastic lesion to be associated with the increased number of infiltrated macrophages (Figure 1F). Moreover, the number of Ki-67-positive proliferating cells increased in the dysplastic mucosa when compared with that in the adjacent normal region (Figure 1D and J). The mean Ki-67 labelling indices in the dysplastic lesions and normal mucosa were 43 and 15%, respectively ($P=0.007$). We also confirmed by BrdU incorporation analysis that cell proliferation was increased in dysplastic lesions (Figure 1G). On the basis of these results, we hypothesized that macrophage infiltration by inflammatory responses causes promotion of Wnt/β-catenin signalling activity in gastric epithelial cells, which probably leads to dysplastic changes in the gastric mucosa.

Requirement of macrophages for intestinal tumour development in $Apc^{\Delta 716}$ mice

To examine whether infiltrated macrophages are required for tumorigenesis, we performed crossing experiments using *op/op* mice, in which the number of macrophages significantly decreased in the majority of tissues because of *Csf1* mutation (Cecchini *et al*, 1994). We first examined whether *op/op* mutation suppressed macrophage infiltration in the inflamed stomach using *K19-C2mE* mice, which develop gastritis with heavy macrophage accumulation (Oshima *et al*, 2004). However, mucosal macrophages were still found in the stomach of the *K19-C2mE op/op* compound mice (Supplementary Figure 1). We therefore crossed *op/op* mice with $Apc^{\Delta 716}$ mice, a model for intestinal polyposis caused by Wnt activation (Oshima *et al*, 1995). $Apc^{\Delta 716}$ mice develop numerous polyps in entire intestinal tract (Figure 2A), and macrophages were infiltrated in the polyp stroma (Figure 2B). Interestingly, $Apc^{\Delta 716}$ *op/op* compound mice showed dramatic suppression of intestinal polyposis (Figure 2C and E), and macrophages were not found in the polyp tissues (Figure 2D). Moreover, the number of polyps >1 mm significantly decreased in $Apc^{\Delta 716}$ *op/op* compound mice by 80% compared with $Apc^{\Delta 716}$ mice. Although it remains to be elucidated as to whether the loss of the CSF-1 function affects tumorigenesis, these results suggest that macrophages were required for the growth of Wnt/β-catenin-activated tumour cells. Consistently, the BrdU labelling index also decreased in $Apc^{\Delta 716}$ *op/op* mouse tumours (Figure 2F).

Fluctuation of Wnt/β-catenin signalling activity in gastric cancer cells

We next examined the regulation of the Wnt/β-catenin signalling activity by *in vitro* experiments using human gastric cancer cells, AGS and Kato-III. AGS cells harbour a heterozygous mutation in the β-catenin gene (*CTNNB1*) at codon 34 (Caca *et al*, 1999; Supplementary Figure 2), whereas *CTNNB1* is amplified in Kato-III cells (Suriano *et al*, 2005). Consistent with the previous results (Nojima *et al*, 2007), both cell lines showed an elevated β-catenin/TCF transcriptional activity as detected by a TOPFLASH assay (Supplementary Figure 3). By immunocytochemistry, the cytoplasmic and nuclear accumulation of β-catenin was found in both AGS and Kato-III cells (Figure 3A, left). We also found the nuclear localization of active form of β-catenin, unphosphorylated on Ser37 and Thr41 (van Noort *et al*, 2002; Figure 3A, right), thus indicating the activation of Wnt/β-catenin signalling. However, several cells showed a weak β-catenin staining intensity (Figure 3A, arrowheads), suggesting that the level of Wnt/β-catenin signalling activity varies in populations.

To examine the Wnt/β-catenin activity in the live cells, we transfected a TOPEGFP vector that expressed a green fluorescent protein (GFP) in response to β-catenin/TCF transcriptional activity (Figure 3B), and established AGS–GFP and Kato-III–GFP cell lines. We confirmed that GFP expression was induced in β-catenin accumulated cells after the transient transfection of mutant *CTNNB1* (S33A) expression vector (Figure 3C). Importantly, we directly found by time-lapse video analysis that the Wnt/β-catenin activity was not constant but fluctuated in individual AGS–GFP cells (Supplementary Video 1).

To confirm the fluctuation of Wnt/β-catenin activity, we isolated by cell sorting the high-GFP (top 5%) and low-GFP (bottom 5%) populations corresponding to high and low Wnt/β-catenin signalling activity, respectively, from AGS–GFP and Kato-III–GFP cells (Figure 3D, left). Immediately after isolation, both populations showed distinct GFP

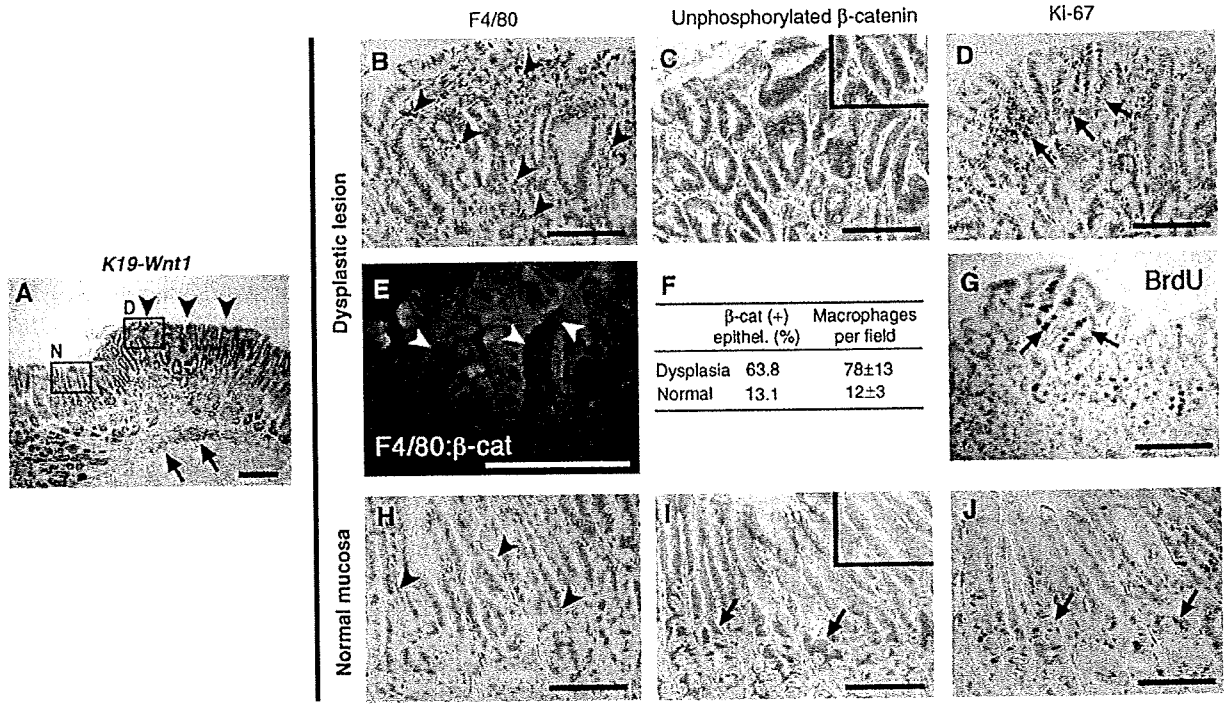

Figure 1 Macrophage accumulation and nuclear localization of β-catenin in dysplastic lesion of the *K19-Wnt1* mouse stomach. (**A**) Representative histology of a dysplastic lesion in the *K19-Wnt1* glandular stomach (H&E staining). The arrowheads indicate the dysplastic mucosal area. The arrows indicate submucosal inflammatory infiltration. High-magnifications of boxed area (D, dysplastic lesion; and N, adjacent normal mucosa) in serial sections are shown in (**B–E, G**) and (**H–J**), respectively. Immunostaining results for macrophage marker F4/80 (B, H), β-catenin (C, I), Ki-67 (D, J), and BrdU (G) are shown. The arrowheads in (B, H) indicate mucosal macrophages. The inset in (C) indicates the nuclear localization of β-catenin in epithelial cells, whereas the inset in (I) indicates weak cytoplasmic accumulation of β-catenin. The arrows in (D, G) indicate proliferating cells that are positive for Ki-67 and BrdU, respectively. (E) Double immunofluorescence staining for F4/80 (red) and β-catenin (green) in dysplastic lesion. Arrowheads indicate macrophages. (**F**) The mean ratio of β-catenin-accumulated epithelial cells and the mean number of infiltrated macrophages per field in the dysplastic lesion and adjacent normal mucosa. The arrows in (I, J) indicate normal progenitor cells localized in gland neck with mild accumulation of β-catenin and positive Ki-67 staining. Bars indicate 100 μm.

intensities (Figure 3D, centre). Importantly, however, the GFP intensities of the isolated populations returned to a similar distribution to the unsorted cells after culturing for 5 days (Figure 3D, right). These results confirmed that the activation level of Wnt/β-catenin signalling fluctuates in each cell.

We next examined the level of Wnt/β-catenin activity in cell cycle-synchronized Kato-III–GFP cells. However, the ratio of a high-GFP population did not change during cell cycling, thus indicating Wnt/β-catenin fluctuation to be independent of the cell cycle status (Supplementary Figure 4).

Promotion of Wnt/β-catenin activity in gastric cancer cells by activated macrophages and TNF-α

We next examined whether the activity of Wnt/β-catenin signalling is promoted by activated macrophages using the GFP reporter-transfected cells. We prepared a conditioned medium of macrophage cell line, RAW264, activated with lipopolysaccharide (LPS) for 24 h; (hereafter, CM-LPS (+)). A conditioned medium from unstimulated RAW264 cells was used as the control (CM-LPS (−)). When AGS–GFP and Kato-III–GFP cells were stimulated with CM-LPS (+), the high-GFP population (corresponding to top 2% in the untreated control cells) significantly increased in a CM concentration-dependent manner (Figure 4A and B, left and top, red area). In contrast, stimulation of the cells with CM-LPS (−) or LPS alone did not affect the Wnt/β-catenin activity in either cell line (Figure 4A and B, middle and bottom). These results indicate that the soluble factor(s) derived from activated macrophages promote the Wnt/β-catenin activity in gastric cancer cells.

TNF-α is a key mediator for inflammation and is produced by activated macrophages. Notably, treatment of the cells with a neutralizing antibody against TNF-α significantly suppressed the effect by CM-LPS (+) to enhance the Wnt/β-catenin activity in both cell lines (Figure 4C). Furthermore, direct treatment with TNF-α increased the level of Wnt/β-catenin activity (Figure 4D). We detected the expression of both TNF R1 and TNF R2 on AGS and Kato-III cells as well as in the primary cultured gastric epithelial cells (Supplementary Figure 5A and C and data not shown). Importantly, the blockade of either receptor by neutralizing antibody significantly suppressed the TNF-α-induced Wnt/β-catenin activation (Supplementary Figure 5B). These results suggest that TNF-α signalling through both TNF R1 and TNF R2 is thus involved in the promotion of the Wnt/β-catenin activity. By immunohistochemistry, we found most TNF-α-expressing cells in gastric tumours to be macrophages, whereas CD11c-positive dendritic cells were rarely detected (Supplementary Figure 6A). Importantly, treatment of the *K19-Wnt1* mice with anti-TNF-α-neutralizing antibody resulted in a decrease of the β-catenin immunostaining intensity in the dysplastic lesions (Supplementary Figure 6B).

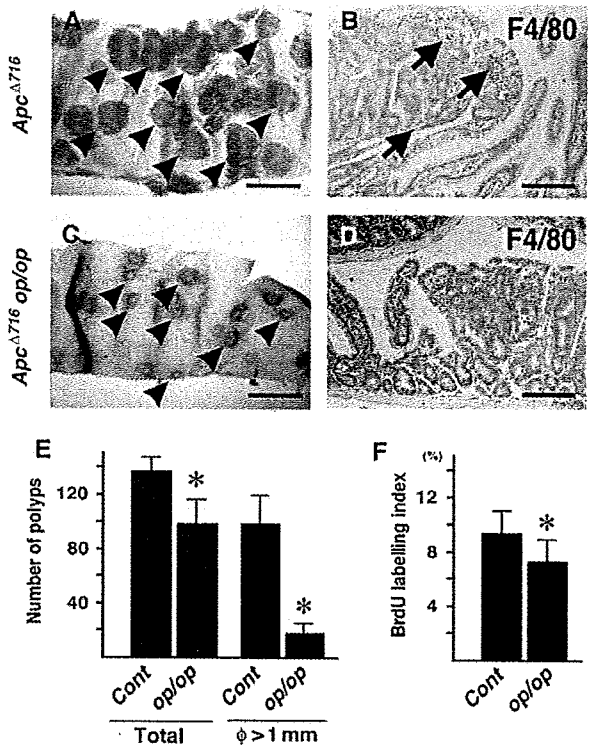

Figure 2 Suppression of intestinal tumorigenesis by depletion of macrophages. (**A**, **C**) Representative photographs of small intestine of $Apc^{\Delta 716}$ mice (A) and $Apc^{\Delta 716}$ *op/op* compound mutant mice (C) were taken using a dissecting microscope. The arrowheads indicate intestinal polyps. Bars indicate 2 mm. (**B**, **D**) F4/80 macrophage immunostaining of polyp tissues in $Apc^{\Delta 716}$ (B) and $Apc^{\Delta 716}$ *op/op* compound mice (D). The arrows indicate macrophages. Bars indicate 100 μm. (**E**) The number of total polyps and large polyps >1 mm in diameter of $Apc^{\Delta 716}$ (*Cont*) and $Apc^{\Delta 716}$ *op/op* compound mice (*op/op*) are shown as mean ± s.d. (**F**) BrdU labelling index in polyps of $Apc^{\Delta 716}$ (*Cont*) and $Apc^{\Delta 716}$ *op/op* mice (*op/op*) are shown as mean ± s.d. $^*P<0.05$ in comparison to the control.

Moreover, we examined the Wnt-promoting effect of other inflammatory cytokines, IL-1β, IL-6 and IL-11, which have an important function in gastric tumorigenesis (Howlett *et al*, 2005; Fox and Wang, 2007). However, these cytokines did not promote Wnt/β-catenin activity in gastric cancer cells, although IL-1β slightly increased the high-GFP population in AGS–GFP cells (Supplementary Figure 7). These results, taken together, suggest that TNF-α is one of the important macrophage-derived factors that promote the Wnt/β-catenin activity in gastric epithelial cells and cancer cells.

Suppression of β-catenin phosphorylation by TNF-α through the inhibition of GSK3β in gastric cancer cells

By a flow cytometry analysis, we found that the level of unphosphorylated β-catenin increased significantly in Kato-III cells when cells were treated with CM-LPS (+) or TNF-α (Figure 5A). By western blotting, we confirmed the increased level of unphosphorylated β-catenin in Kato-III cells stimulated with CM-LPS (+) or TNF-α (Figure 5B). These results suggested that CM-LPS (+) or TNF-α suppressed the phosphorylation of β-catenin, resulting in Wnt/β-catenin promotion. Significantly, treatment with TNF-α resulted in an increase of GSK3β phosphorylation on Ser9 both in AGS and Kato-III cells (Figure 5C), which caused the suppression of the GSK3β activity (Cross *et al*, 1995). The mean relative band intensities of the phosphorylated GSK3β to the control level were 2.03 ± 0.14 ($P=0.009$) and 1.68 ± 0.31 ($P=0.03$) in the AGS and Kato-III cells, respectively. Interestingly, a strong immunostaining signal for phosphorylated GSK3 was found in a sub-population of Kato-III cells that also showed nuclear accumulation of β-catenin at the same time (Figure 5D). These results suggest that the promotion of Wnt/β-catenin signalling is regulated by the GSK3β phosphorylation status in gastric cancer cells. Akt is an important kinase for phosphorylation of GSK3β at Ser9 (Sharma *et al*, 2002). Importantly, the active form of Akt, phosphorylated on Ser473, increased significantly after TNF-α stimulation in both AGS and Kato-III cells (Figure 5C). The mean relative band intensities of the phosphorylated Akt to the control level were 2.08 ± 0.16 ($P=0.005$) and 1.81 ± 0.19 ($P=0.002$) in the AGS and Kato-III cells, respectively. These results suggest that TNF-α accelerates the GSK3β phosphorylation through the activation of the Akt pathway.

NF-κB-independent promotion of Wnt/β-catenin activity in gastric cancer cells

To examine whether NF-κB is involved in Wnt/β-catenin promotion by activated macrophages, we transfected IκB-superrepressor (IκBSR) expression vector into AGS–GFP cells and established two sublines, in which TNF-α-induced NF-κB activation was suppressed (Figure 6A). Notably, the TNF-α- or CM-LPS (+)-induced promotion of the Wnt/β-catenin activity did not change in either of IκBSR-transfected AGS–GFP cells (Figure 6B), thus suggesting the existence of an NF-κB-independent mechanism for the TNF-α-induced Wnt/β-catenin promotion.

When Kato-III cells were treated with the protein synthesis inhibitor cycloheximide, the unphosphorylated β-catenin-positive population decreased gradually in an incubation time-dependent manner, probably due to the phosphorylation of β-catenin by GSK3β (Figure 6C, black lines). However, the simultaneous treatment with CM-LPS (+) significantly suppressed the cycloheximide-induced decrease of this population (Figure 6C, red lines). Therefore, it is also possible that activated macrophages suppress β-catenin phosphorylation independent of protein synthesis, which is consistent with the results that the transcription factor NF-κB pathway is not involved in the suppression of β-catenin phosphorylation.

Macrophage infiltration and Wnt/β-catenin activation in mouse gastric epithelial cells by Helicobacter infection

We next examined whether Wnt/β-catenin signalling is activated by infection-associated inflammation in the mouse stomach. *H. felis*, a close relative of *H. pylori* was infected into *K19-Wnt1* mouse stomach. At 8 weeks after *H. felis* infection, the infiltration of macrophages was found in the *H. felis*-infected gastric mucosa (Figure 7A–C), whereas tissue macrophages were sparsely scattered in the non-infected mucosal area (Figure 7G–I). Such an inflamed mucosa in the infected *K19-Wnt1* mice was only detected by histological examinations, and this inflamed mucosa was distinct from the spontaneously developed dysplastic lesions (Figure 1A).

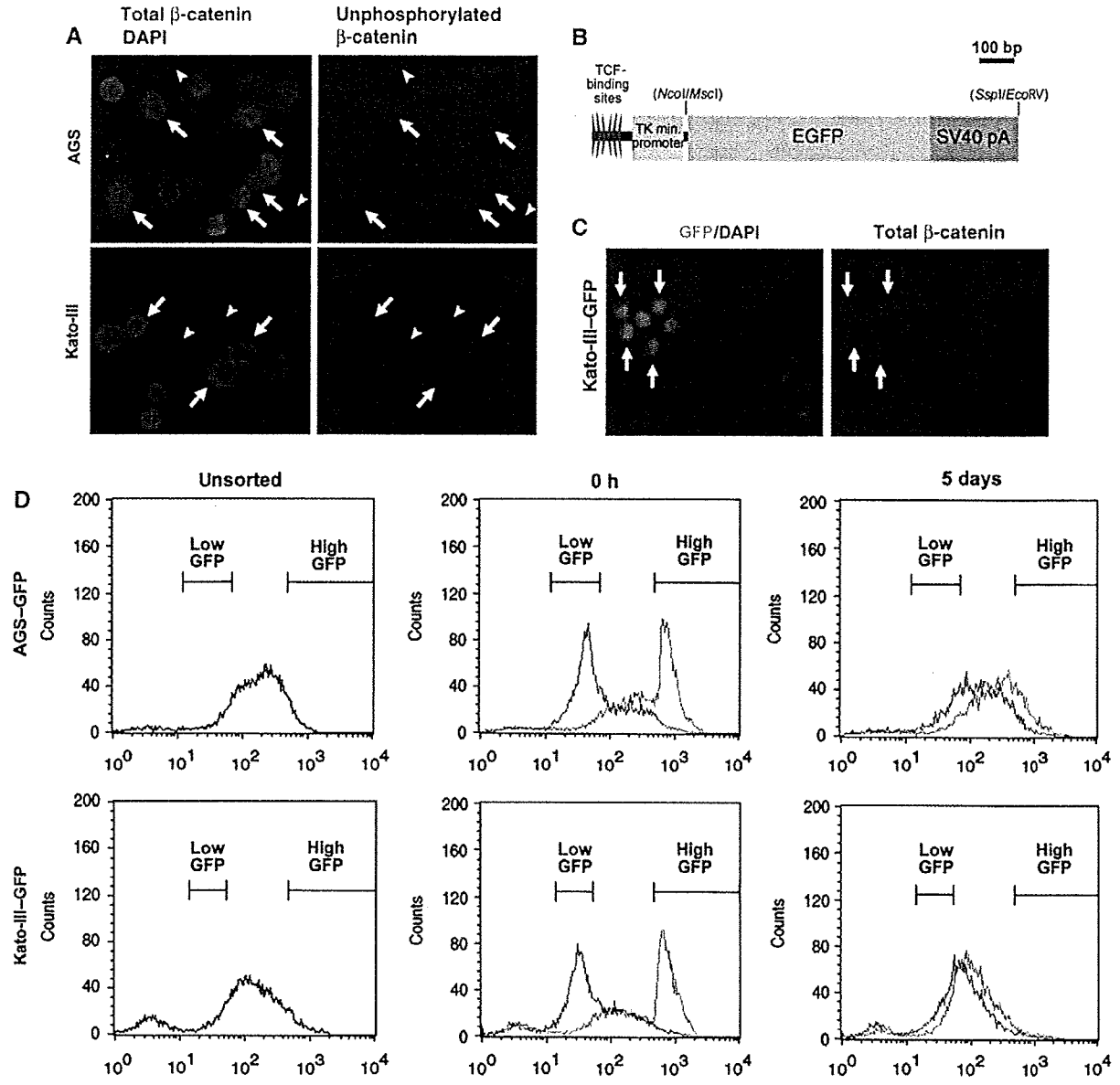

Figure 3 Fluctuation of the Wnt/β-catenin activity in gastric cancer cells. (**A**) Representative results of immunocytochemistry of AGS (top panels) and Kato-III (bottom panels) using anti-total β-catenin antibody (green) and DAPI (blue) (left panels) or anti-unphosphorylated β-catenin antibody (red) (right panels) of the same specimen. The arrows indicate cells with accumulated both total and unphosphorylated β-catenin. The arrowheads indicate cells with weak or loss of β-catenin staining. (**B**) Construction of TOPEGFP expression vector. EGFP cDNA was inserted between TCF-binding site/TK minimum promoter and SV40 pA signal. (**C**) Representative results of immunocytochemistry of Kato-III–GFP cells transiently transfected with pcDNA3-S33A-β-catenin for 72 h. GFP expression (green) with DAPI staining (blue) (left panel), and unphosphorylated β-catenin (red) of the same specimen (right panel) are shown. The arrows indicate the cell cluster with elevated GFP and unphosphorylated β-catenin levels. (**D**) Representative results of flow cytometry for GFP fluorescence of AGS–GFP (top) and Kato-III–GFP (bottom) cells. Flow cytometry results of the isolated high-GFP (top 5%, red line) and low-GFP (bottom 5%, blue line) populations at 0 h (centre) and 5 days (right) after isolation by cell sorting.

Importantly, the number of β-catenin-accumulated epithelial cells increased significantly in the infected and inflamed mucosa compared with that in the non-inflamed mucosa (Figure 7D, J and M). These results suggest that the infection-associated inflammation promotes the Wnt/β-catenin signalling activity in gastric epithelial cells *in vivo*. Moreover, in the inflamed mucosa, the epithelial cell proliferation detected by Ki-67 immunostaining significantly increased (Figure 7E, K and N). Furthermore, the number of H^+/K^+-ATPase-positive parietal cells decreased dramatically in the *H. felis*-infected area, thus indicating the suppression of epithelial differentiation (Figure 7F, L and O). These results, taken together, suggest that infiltrated macrophages in response to *Helicobacter* infection have an important function in the activation of Wnt/β-catenin signalling, thereby enhancing the proliferation and suppression of differentiation. When $Apc^{\Delta 716}$ mice were infected with *H. felis*, we did not find any β-catenin-accumulated dysplastic cells in the

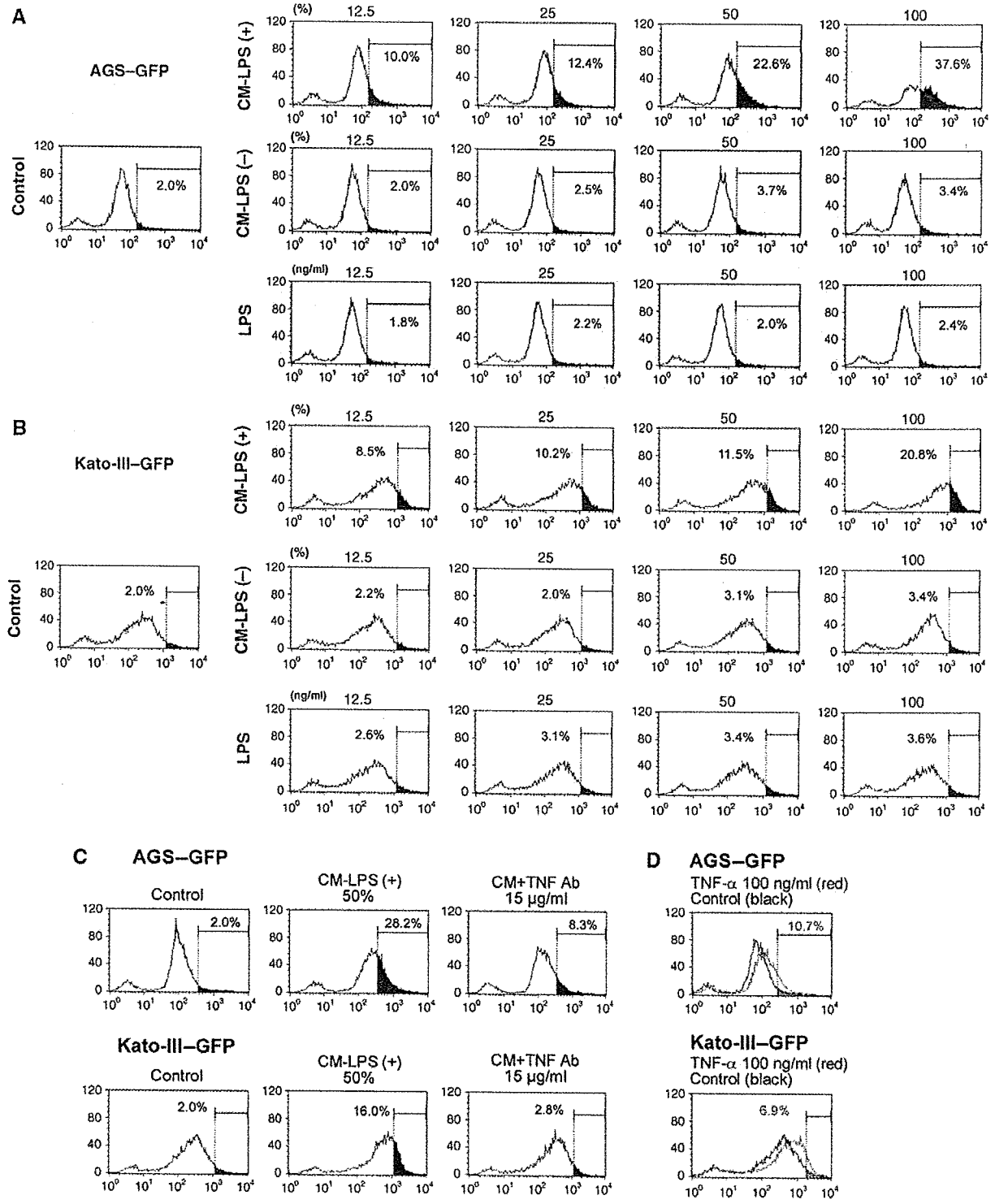

Figure 4 Enhancement of Wnt/β-catenin signalling by the activated macrophages in gastric cancer cells. (**A**, **B**) Representative results of flow cytometry of AGS-GFP (A) and Kato-III-GFP cells (B). The cells were treated with CM-LPS (+) (top), CM-LPS (−) (middle) or LPS alone (bottom) at various concentrations indicated on top of each panel. The red area in each panel indicates a population with a high GFP intensity corresponding to the top 2% of the control cells (left). The percentage of high-GFP population (red area) is indicated in each panel. (**C**) Representative flow cytometry of AGS-GFP (top) and Kato-III-GFP (bottom) treated with CM-LPS (+) alone (centre) or CM-LPS (+) with anti-TNF-α-neutralizing antibody (right). The percentage of a high-GFP population (red area corresponding to top 2% in control cells, left) is indicated in each panel. (**D**) Representative flow cytometry results of AGS-GFP (top) and Kato-III-GFP (bottom) treated with TNF-α (red lines) and untreated control (black lines). The percentage of high GFP in TNF-α-treated cells (corresponding to top 2% in control cells, grey area) is indicated in each panel.

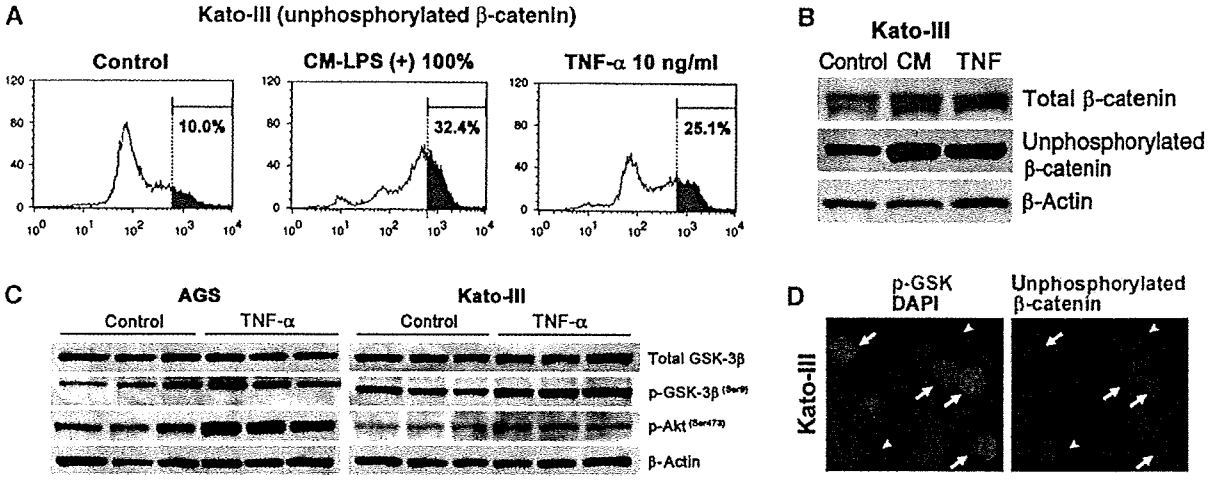

Figure 5 Suppression of β-catenin phosphorylation by CM-LPS (+) or TNF-α in gastric cancer cells. (A) Representative flow cytometry results of Kato-III cells using an antibody against unphosphorylated β-catenin on Ser37 and Thr41 are shown. The cells were treated with CM-LPS (+) (centre) or TNF-α (right) for 24 h. The red area indicates population with high level of unphosphorylated β-catenin: top 10% in control cells (left). The percentage of red area is indicated in each panel. (B) Western blotting of Kato-III cells for total β-catenin (top) and unphosphorylated β-catenin (middle). The cells were treated with CM-LPS (+) (CM) or TNF-α at 10 ng/ml (TNF). β-Actin was used as an internal control (bottom). (C) Western blotting of AGS cells (left) and Kato-III cells (right) for total and phosphorylated GSK3β on Ser9, and phosphorylated Akt on Ser473. β-Actin was used as an internal control. The cells were treated with TNF-α at 100 ng/ml (TNF) in serum-free conditions. The results of three independent samples are shown for each cell line. (D) Representative immunocytochemistry for phosphorylated GSK3 (p-GSK, green) and DAPI (blue) (left) and unphosphorylated β-catenin (red) (right) of the same specimen. The arrows indicate cells with strong staining for both p-GSK and β-catenin, whereas the arrowheads indicate cells with weak staining for both.

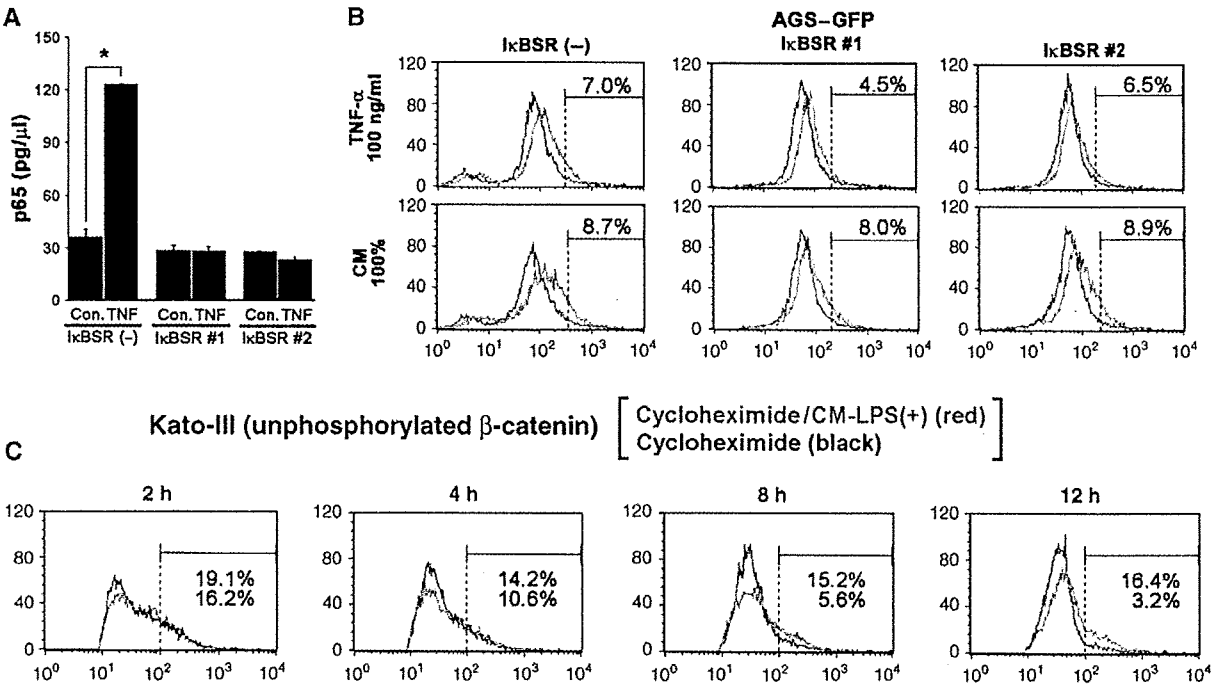

Figure 6 NF-κB-independent promotion of the Wnt/β-catenin signalling activity. (A) The level of NF-κB activity in the TNF-α-treated (TNF) or untreated control (Con.) cells (mean ± s.d.). IκBSR nos. 1 and 2 are AGS–GFP-derived stable transfectants with IκBSR, whereas IκBSR (−) indicates parental AGS–GFP. (B) Representative flow cytometry results of IκBSR(−), IκBSR nos. 1 and 2 cells (left to right) treated with TNF-α (top) or CM-LPS (+) (bottom) at the indicated concentrations (red lines). The percentage of high-GFP populations (corresponding to top 2% in untreated cells, black lines) is indicated in each panel. (C) Flow cytometry results of Kato-III cells using antibody against unphosphorylated β-catenin. The cells were treated with cycloheximide alone (black line) or cycloheximide and CM-LPS (+) (red line) for 2, 4, 8 and 12 h. The percentages of the population with high level of unphosphorylated β-catenin are indicated in each panel (red, cycloheximide and CM-LPS (+); black, cycloheximide alone).

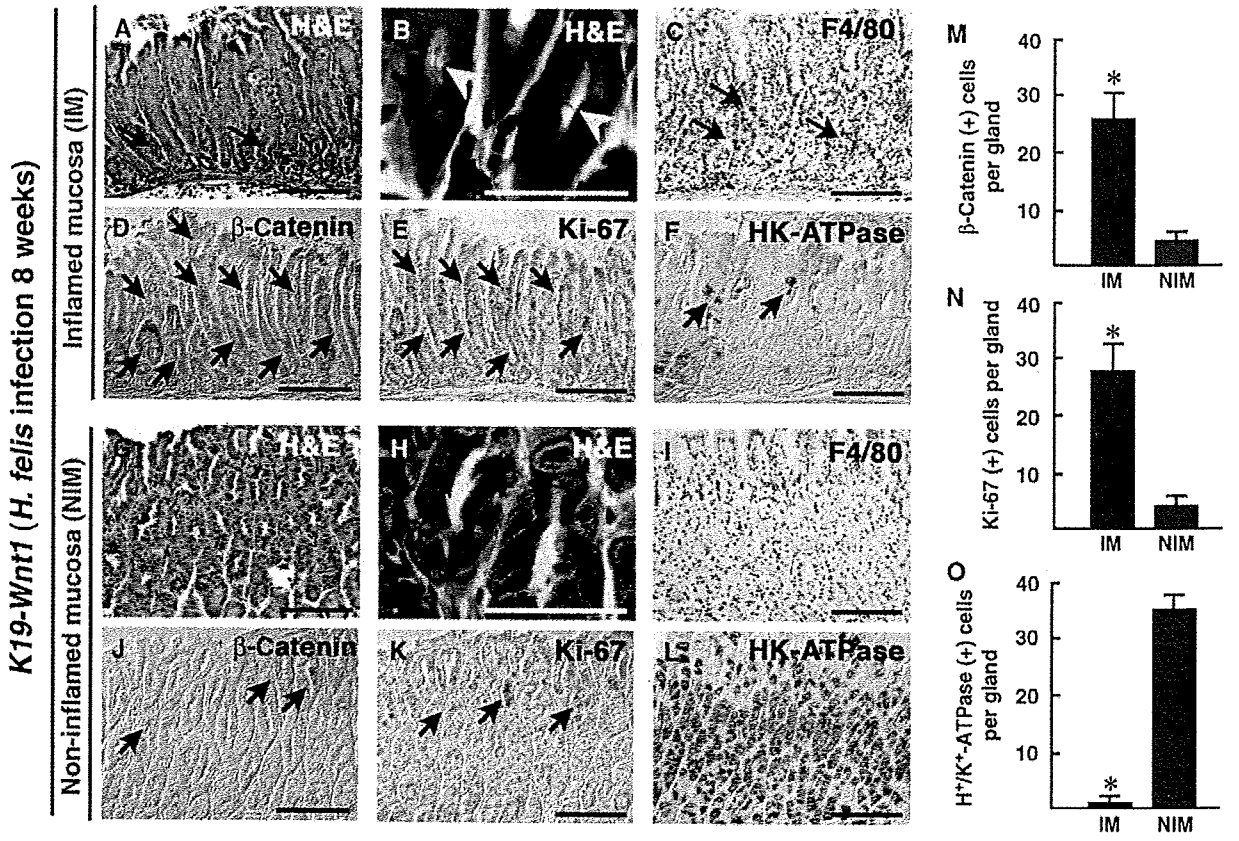

Figure 7 The activation of Wnt/β-catenin signalling in *H. felis*-infected gastric mucosa of *K19-Wnt1* mice. (**A–F**) Representative histology of inflamed gastric mucosa (IM) of *K19-Wnt1* mice infected with *H. felis* for 8 weeks. (**G–L**) Non-inflamed gastric mucosal (NIM) area of the *K19-Wnt1* mice. H&E staining (A, G), high magnified H&E staining (B, H), immunostaining for F4/80 (C, I), unphosphorylated β-catenin (D, J), Ki-67 (E, K) and H^+/K^+-ATPase (F, L). Bars in (B, H) and other panels indicate 50 and 100 μm, respectively. The arrows in (A, C) indicate infiltrated mononuclear cells and macrophages, respectively. The yellow arrowheads in (B) indicate *Helicobacter* bacteria in the gland lumen, which is not found in NIM (H). The arrows in (D, E) indicate β-catenin-accumulated and proliferating epithelial cells, respectively. The arrows in (F) indicate H^+/K^+-ATPase-positive parietal cells that are dramatically decreased in IM compared with NIM (L). The arrows in (J, K) indicate progenitor cells with cytoplasmic β-catenin accumulation and Ki-67-positive proliferation, respectively. The mean numbers of positive cells per gland for unphosphorylated β-catenin (**M**), Ki-67 (**N**), and H^+/K^+-ATPase (**O**) in IM (red bars) and NIM (blue bars) are shown as histograms (mean ± s.d.). The asterisks indicate $P<0.05$.

inflamed gastric mucosa (data not shown). Therefore, it is possible that the basal activation level of Wnt/β-catenin signalling is required for its promotion.

Tumour development in H. felis-infected K19-Wnt1 mouse stomach

We finally examined whether *H. felis* infection contributes to gastric tumorigenesis in *K19-Wnt1* mice. Importantly, *K19-Wnt1* mice developed gastric tumours at 20 weeks after *H. felis* infection, whereas no tumours were found in the *H. felis*-infected wild-type mice (Figure 8A and E). Histologically, submucosal infiltration was found in both *H. felis*-infected *K19-Wnt1* and wild-type mouse stomach (Figure 8B and F). Although macrophage infiltration was detected in both genotypes (Figure 8C and G), dysplastic epithelial cells were evident in the infected *K19-Wnt1* tumours but not in the wild-type mouse stomach (Figure 8D and H). These results, taken together, suggest that infection-associated inflammation has an important function in gastric tumorigenesis through the promotion of the Wnt/β-catenin activity beyond the basal activation level.

Discussion

Macrophage infiltration and cancer development, progression and stemness

The activation of Wnt/β-catenin signalling by genetic alteration, such as mutation in *APC* or *CTNNB1*, is responsible for gastrointestinal tumorigenesis. However, accumulating evidence suggests that further promotion of the Wnt/β-catenin activity has an important function in tumour growth and progression (Fodde and Brabletz, 2007). For example, increased β-catenin accumulation is found in the invasion front of colon cancer (Brabletz *et al*, 1998). We herein demonstrated direct evidence that the Wnt/β-catenin activity fluctuates in individual cancer cells that carry the same genetic alteration in *CTNNB1*. Accordingly, Wnt/β-catenin signalling can be promoted beyond the basal activated level caused by genetic alteration, and such promotion may have an important function in both tumour development and progression.

We have previously shown the induction of COX-2/PGE_2 pathway to have an important function in the intestinal tumorigenesis that is triggered by Wnt/β-catenin activation (Oshima *et al*, 1996; Sonoshita *et al*, 2001). The simultaneous

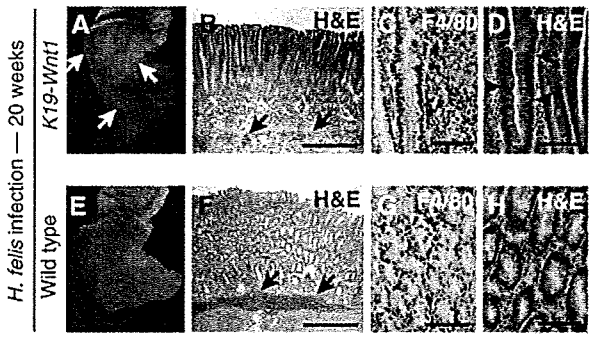

Figure 8 Tumour development in *H. felis*-infected *K19-Wnt1* mouse stomach. *K19-Wnt1* (**A–D**) and wild-type (**E–H**) mouse stomach infected with *H. felis* for 20 weeks. (A, E) Macroscopic photographs. The arrows in (A) indicate gastric tumours that developed in the infected *K19-Wnt1* mice. H&E staining at low magnification (B, F) and high magnification (D, H). Immunostaining results for macrophage marker F4/80 (C, G). The arrows in (B, F) indicate submucosal infiltration. The arrowheads in (D) indicate dysplastic epithelial cells. Bars in (B, F) and (C, D, G, H) indicate 200 and 40 μm, respectively.

induction of both Wnt and PGE_2 pathways is also responsible for gastric tumour development in mouse models (Oshima *et al*, 2006). Although PGE_2 may have multiple functions for tumorigenesis, we previously found an increased PGE_2 level to result in macrophage accumulation in the gastric mucosa of *K19-C2mE* mice (Oshima *et al*, 2004). Accordingly, it is possible that macrophage infiltration in dysplastic lesions of *K19-Wnt1* mice is caused by the spontaneous induction of COX-2/PGE_2 pathway. We herein show that Wnt/β-catenin signalling is promoted by macrophage-derived TNF-α, which contributes to gastric tumorigenesis. It is therefore possible that the induction of the COX-2/PGE_2 pathway promotes Wnt/β-catenin signalling through the enhancement of macrophage infiltration, which is responsible for tumour development.

On the other hand, Wnt/β-catenin signalling is not activated in the stomach of either *K19-C2mE* mice or *H. felis*-infected $Apc^{\Delta 716}$ mice, thus indicating that the induction of the COX-2/PGE_2 pathway and subsequent macrophage infiltration are not sufficient for the promotion of Wnt/β-catenin in gastric epithelial cells. It is conceivable that the basal activation of the Wnt/β-catenin pathway by genetic alteration is required for the promotion of Wnt/β-catenin signalling.

The activation of Wnt/β-catenin pathway is also suggested to be important for stemness. Wnt/β-catenin signalling is required for the maintenance of normal intestinal stem cells (Korinek *et al*, 1998), and the increase in the Wnt/β-catenin activity contributes to the maintenance of stemness in ES cells (Kielman *et al*, 2002). Accordingly, it is possible that the increased Wnt/β-catenin activity is also important for the maintenance of cancer stem cells. Therefore, infiltrated macrophages in tumour tissues may be an important component of niche for cancer stem cells by promoting Wnt/β-catenin signalling through TNF-α pathway. This hypothesis is supported by the results that macrophages are required for the maintenance of progenitor cells in the intestinal crypt (Pull *et al*, 2005).

Possible pathways other than TNF-α for the promotion of the Wnt/β-catenin signalling activity

It has been shown that inflammatory cytokines, TNF-α, IL-1β, IL-6 or IL-11, have an important function in gastric tumorigenesis (Howlett *et al*, 2005; Fox and Wang, 2007). Among these cytokines, TNF-α is the most potent Wnt/β-catenin-promoting factor, although IL-1β slightly increases Wnt signalling in AGS cells. However, the increased level of the Wnt/β-catenin activity by CM-LPS (+) is significantly higher than that by TNF-α alone in both cell lines (Figure 4), thus suggesting the effect of other macrophage-derived factors on Wnt/β-catenin promotion. It has been reported that hepatocyte growth factor activates Wnt/β-catenin signalling through the tyrosine phosphorylation of β-catenin (Rasola *et al*, 2006), and platelet-derived growth factor also promotes Wnt/β-catenin signalling through suppression of β-catenin phosphorylation (Yang *et al*, 2006). It is therefore possible that these factor(s) contribute to Wnt/β-catenin promotion together with TNF-α in gastric tumorigenesis.

Recently, using a colon tumour mouse model, TNF R1 signalling in bone marrow-derived cells has been shown to indirectly enhance epithelial Wnt/β-catenin signalling (Popivanova *et al*, 2008). Accordingly, it is possible that TNF-α signalling, not only in epithelial cells but also in stromal cells, may therefore contribute to the promotion of Wnt/β-catenin signalling in cancer cells.

Promotion of Wnt/β-catenin signalling in cancer cells that retain wild-type CTNNB1

We show here that TNF-α stimulation promotes the Wnt/β-catenin signalling activity through the suppression of β-catenin phosphorylation by GSK3β. Therefore, the expression of wild-type β-catenin is required for the promotion of Wnt/β-catenin signalling in epithelial cells as well as cancer cells. Because Kato-III cells have a multicopy of the wild-type *CTNNB1* (Suriano *et al*, 2005), TNF-α stimulation suppresses phosphorylation of these β-catenin, thus leading to the enhancement of Wnt/β-catenin signalling. On the other hand, AGS cells possess mutation in *CTNNB1* close to the phosphorylation site of GSK3β (Supplementary Figure 2; Caca *et al*, 1999), which causes the activation of the basal Wnt/β-catenin signalling. It is therefore possible that TNF-α stimulation suppresses phosphorylation of wild-type β-catenin expressed from retained intact *CTNNB1*, which contributes to the promotion of the total Wnt/β-catenin activity of AGS cells. In human gastric cancer, a *CTNNB1* mutation is found in about 30% of the Wnt-activated cases (Clements *et al*, 2002). However, either a somatic mutation or downregulation of E-cadherin (Cheng *et al*, 2005), secreted frizzled-related proteins (Nojima *et al*, 2007), or β-TrCP, a component of ubiquitin ligase complex (Kim *et al*, 2007) is found in gastric cancer, which leads to the basal activation of Wnt/β-catenin signalling without mutation in *CTNNB1*. These results, taken together, suggest that wild-type β-catenin expressed in gastric cancer cells is stabilized by inflammatory macrophages, thus resulting in the promotion of Wnt/β-catenin signalling, which contributes to cancer development, progression and the maintenance of cancer stem cells.

Accordingly, the present results suggest that the suppression of macrophage infiltration and its activation by anti-inflammatory drugs or inhibitors for PGE_2 pathway is, therefore, a possible strategy for chemoprevention against gastric cancer.

Materials and methods

Animal experiments

The construction of *K19-Wnt1* and *K19-C2mE* transgenic mice has been described previously (Oshima *et al*, 2004, 2006). Briefly, *K19-Wnt1* mice express *Wnt1*, whereas *K19-C2mE* mice express COX-2 and mPGES-1 in gastric epithelial cells under transcriptional regulation by cytokeratin 19 (K19) gene promoter. *K19-Wnt1* transgenic mice were euthanized at 30 weeks of age ($n=10$), and the glandular stomach was fixed with 4% paraformaldehyde and processed for histological analysis. *H. felis* (ATCC49179) was cultured as previously described (Oshima *et al*, 2004). *H. felis* bacteria were inoculated at 10^8 per mouse p.o. into *K19-Wnt* mice, $Apc^{\Delta 716}$ mice (Oshima *et al*, 1995) and wild-type mice. The infected *K19-Wnt1* mice were examined at 8 and 20 weeks after the *H. felis* inoculation ($n=3$ for each mice). The infected $Apc^{\Delta 716}$ mice were examined at 6 weeks after infection ($n=4$). The localization of *H. felis*-infected mucosa at 8 weeks was estimated by the detection of bacteria using microscope with × 100 objective (Figure 7B). $Apc^{\Delta 716}$ mice were crossed with *op/op* mice (The Jackson Laboratory) to obtain $Apc^{\Delta 716}$ *op/op* compound mice ($n=3$) and littermate control $Apc^{\Delta 716}$ mice ($n=3$). The intestine of $Apc^{\Delta 716}$ and $Apc^{\Delta 716}$ *op/op* mice was examined at 12 weeks of age, and the total number of polyps was determined using a dissecting microscope. For scoring the BrdU labelling index, the mice were injected i.p. with 200 μl of BrdU solution (Roche) and then the tissue specimens were processed for immunostaining using anti-BrdU antibody. All animal experiments were carried out according to the protocol approved by the Committee on Animal Experimentation of Kanazawa University.

Histology and immunostaining

The stomach tissues were fixed in 4% paraformaldehyde, paraffin-embedded and sectioned at 4 μm thickness. These sections were stained with H&E. Serial sections were immunostained with antibodies for Ki-67 (DakoCytomation), F4/80 (Serotec), unphosphorylated (activated) β-catenin on Ser37 and Thr41 (Upstate), H^+/K^+-ATPase (MBL, Nagoya, Japan) or BrdU (BD Biosciences) as the primary antibody. The staining signals were visualized using the Vectorstain Elite Kit (Vector Laboratories). The number of positive stained cells for F4/80, β-catenin, Ki-67 or H^+/K^+-ATPase was scored in 20 randomly selected gastric glands and the mean values were calculated. The number of BrdU-positive cells and the total number of nuclei was counted in five microscopic fields and then the mean value was calculated as the BrdU labelling index. For immunofluorescence staining, Alexa Fluor 594 donkey anti-mouse IgG or Alexa Fluor 488 anti-rat or rabbit IgG (Molecular Probes) was used as the secondary antibody.

Plasmid vector construction

For the construction of the β-catenin/TCF reporter plasmid with GFP (TOPEGFP vector), cDNA encoding EGFP was excised from pIRES2-EGFP (Clontech) and replaced with luciferase gene in TOPFLASH plasmid (Upstate). TOPEGFP reporter plasmid was transfected to cells using Effectene Transfection Reagent (Qiagen), and stable cell lines were then obtained by cell sorting. The Wnt/β-catenin activity using TOPEGFP reporter was measured by flow cytometry (see below). pcDNA3-S33A-β-catenin and pBSFI-IκBSR plasmids were kindly provided by Dr Peter Vogt at the Scripps Research Institute. pcDNA3-S33A-β-catenin was transiently transfected to Kato-III–GFP cells for 72 h to express stabilized mutant β-catenin. pBSFI-IκBSR was transfected to AGS–GFP cells to establish the sublines in which the NF-κB pathway is suppressed.

Immunocytochemistry

Gastric cancer cells grown on cover slips were fixed with 10% neutral buffered formalin and permeabilized with 0.1% Triton X-100 in PBS. Anti-total β-catenin antibody (Sigma), anti-unphosphorylated β-catenin antibody (Upstate), or anti-phosphorylated GSK3 (Cell Signaling) was used as the primary antibody, and anti-mouse IgG Alexa 594 or anti-rat IgG Alexa 488 (Molecular Probes) were used as the secondary antibody. Next, cover slips were mounted using VECTASHIELD Mounting Medium (Vector Laboratories) that contained DAPI for nuclear staining.

Cell culture and preparation of conditioned medium

Gastric cancer cell lines, AGS (ATCC) and Kato-III (Cell Resource Center for Biomedical Research, Tohoku University, Japan) were cultured in RPMI1640 medium supplemented with 10% FBS in a humidified incubator at 37°C with 5% CO_2. The mouse macrophage cell line RAW264 (RIKEN BioResource Center, Tsukuba, Japan) was cultured in RPMI1640, and treated with LPS purified from *Salmonella enterica* serotype *typhimurium* (Sigma) at 100 ng/ml for 24 h. The conditioned medium, CM-LPS (+) was collected and used for the Wnt/β-catenin activation experiments. The control conditioned medium, CM-LPS (−) was prepared from non-stimulated RAW264 cell culture. For either the stimulation or inhibition of the TNF-α pathway, TNF-α (Calbiochem) or anti-mouse TNF-α-neutralizing antibody (R&D systems) was added, respectively, in the culture medium at the indicated concentration.

NF-κB ELISA assay

The nuclear extract was prepared from AGS–GFP cells or pBSFI-IκBSR-transfected clones (IκBSR nos. 1 and 2) using NE-PER Nuclear Extraction Reagents (Pierce), and the NF-κB activity was measured using an NF-κB p65 Transcription Factor Assay Kit (Active Motif). These cell lines were also used for the flow cytometry analysis.

Flow cytometry analysis

After treatment with CM-LPS (+), CM-LPS (−), LPS or TNF-α at the indicated concentrations for 48 h, AGS–GFP, Kato-III–GFP cells or pBSFI-IκBSR-transfected cells (IκBSR nos. 1 and 2) were washed with PBS containing 2% FCS and stained with 5 μg/ml propidium iodide to exclude dead cells. GFP fluorescence was examined with FACSCalibur (Becton Dickinson). A fluorescence intensity corresponding to the top 2% of the control untreated cells was judged as the high-GFP population (high-Wnt/β-catenin signalling population).

For the analysis of intracellular unphosphorylated (active) β-catenin, cells were fixed in 1–2% paraformaldehyde and permeabilized using 0.05% Triton X-100 in PBS containing 2% FCS. Next, the cells were incubated with anti-unphosphorylated β-catenin antibody on Ser37 and Thr41 (Upstate) followed by anti-mouse IgG-Alexa 488 (Molecular Probes), and examined with FACSCalibur. For the inhibition of protein translation, the cells were treated with cycloheximide (Sigma) at 0.5 μg/ml for the indicated time, and then the intracellular unphosphorylated β-catenin was measured by a FACS analysis as described above.

Western blotting analysis

For the detection of total β-catenin and unphosphorylated β-catenin, the cells were stimulated with CM-LPS (+) or TNF-α at 10 ng/ml for 24 h. For the detection of total or phosphorylated GSK3β (Ser9), and phosphorylated Akt (Ser473), the cells were cultured in serum-free conditions for 24 h followed by stimulation with TNF-α at 100 ng/ml for 24 h. Next, the cells were lysed and sonicated in lysis buffer. After centrifugation at 20 000 *g*, 10 μg of the supernatant protein was separated in a 10% SDS-polyacrylamide gel. Antibodies for unphosphorylated (active) β-catenin (Upstate), total β-catenin (Sigma), total GSK3β (BD Biosciences), phosphorylated GSK3 on Ser9 and 21 (Cell Signaling), and phosphorylated Akt at Ser473 (Cell Signaling) were used as the primary antibody. β-Actin was used as an internal control. The ECL detection system (Amersham Biosciences) was used to detect specific signals.

Statistical analysis

The data were analysed by the paired or unpaired *t*-test using Microsoft Excel (Microsoft). A value of $P<0.05$ was accepted as statistically significant.

Supplementary data

Supplementary data are available at *The EMBO Journal* Online (http://www.embojournal.org).

Acknowledgements

We thank Manami Watanabe for her valuable technical contribution. This study was supported by Grant-in-Aid for the Third-Term Comprehensive Control Strategy for Cancer from the Ministry of Health, Labour and Welfare of Japan, Grant-in-Aid for Priority Areas from the Ministry of Education, Culture, Sports, Science and Technology of Japan, and Takeda Science Foundation, Japan.

References

Brabletz T, Jung A, Hermann K, Günther K, Hohenberger W, Kirchner T (1998) Nuclear overexpression of the oncoprotein β-catenin in colorectal cancer is localized predominantly at the invasion front. *Pathol Res Pract* **194:** 701–704

Caca K, Kolligs FT, Ji X, Hayes M, Qian J, Yahanda A, Rimm DL, Costa J, Fearon ER (1999) β- and γ-catenin mutations, but not E-cadherin inactivation, underlie T-cell factor/lymphoid enhancer factor transcriptional deregulation in gastric and pancreatic cancer. *Cell Growth Differ* **10:** 369–376

Cecchini MG, Dominguez MG, Mocci S, Wetterwald A, Felix R, Fleisch H, Chisholm O, Hofstetter W, Pollard JW, Stanley ER (1994) Role of colony stimulating factor-1 in the establishment and regulation of tissue macrophages during postnatal development of the mouse. *Development* **120:** 1357–1372

Cheng XX, Wang ZC, Chen XY, Sun Y, Kong QY, Liu J, Li H (2005) Correlation of Wnt-2 expression and β-catenin intracellular accumulation in Chinese gastric cancers: relevance with tumour dissemination. *Cancer Lett* **223:** 339–347

Clements WM, Wang J, Sarnaik A, Kim OJ, MacDonald J, Fenoglio-Preiser C, Groden J, Lowy AM (2002) *β-Catenin* mutation is a frequent cause of Wnt pathway activation in gastric cancer. *Cancer Res* **62:** 3503–3506

Correa P (2003) *Helicobacter pylori* infection and gastric cancer. *Cancer Epidemiol Biomarkers Prev* **12:** 238s–241s

Coussens LM, Werb Z (2002) Inflammation and cancer. *Nature* **420:** 860–867

Cross DA, Alessi DR, Cohen P, Andjelkovich M, Hemmings BA (1995) Inhibition of glycogen synthase kinase-3 by insulin mediated by protein kinase B. *Nature* **378:** 785–789

Fodde R, Brabletz T (2007) Wnt/β-catenin signaling in cancer stemness and malignant behavior. *Curr Opin Cell Biol* **19:** 150–158

Fodde R, Smits R, Clevers H (2001) *APC*, signal transduction and genetic instability in colorectal cancer. *Nat Rev Cancer* **1:** 55–67

Fox JG, Wang TC (2007) Inflammation, atrophy and gastric cancer. *J Clin Invest* **117:** 60–69

Gaspar C, Fodde R (2004) *APC* dosage effects in tumorigenesis and stem cell differentiation. *Int J Dev Biol* **48:** 377–386

Greten FR, Eckmann L, Greten TF, Park JM, Li ZW, Egan LJ, Kagnoff MF, Karin M (2004) IKKβ links inflammation and tumorigenesis in a mouse model of colitis-associated cancer. *Cell* **118:** 285–296

Howlett M, Judd LM, Jenkins B, La Gruta NL, Grail D, Ernst M, Giraud AS (2005) Differential regulation of gastric tumor growth by cytokines that signal exclusively through the coreceptor gp130. *Gastroenterology* **129:** 1005–1018

Kielman MF, Ridanpää M, Gaspar C, van Poppel N, Breukel C, van Leeuwen S, Taketo MM, Roberts S, Smits R, Fodde R (2002) *Apc* modulates embryonic stem-cell differentiation by controlling the dosage of β-catenin signaling. *Nat Genet* **32:** 594–605

Kim CJ, Song JH, Cho YG, Kim YS, Kim SY, Nam SW, Yoo NJ, Lee JY, Park WS (2007) Somatic mutations of the β-*TrCP* gene in gastric cancer. *APMIS* **115:** 127–133

Korinek V, Barker N, Moerer P, van Donselaar E, Huls G, Peters PJ, Clevers H (1998) Depletion of epithelial stem-cell compartments in the small intestine of mice lacking Tcf-4. *Nat Genet* **19:** 379–383

Li Q, Ishikawa TO, Oshima M, Taketo MM (2005) The threshold level of adenomatous polyposis coli protein for mouse intestinal tumorigenesis. *Cancer Res* **65:** 8622–8627

Nojima M, Suzuki H, Toyota M, Watanabe Y, Maruyama R, Sasaki S, Sasaki Y, Mita H, Nishikawa N, Yamaguchi K, Hirata K, Itoh F, Tokino T, Mori M, Imai K, Shinomura Y (2007) Frequent epigenetic inactivation of *SFRP* genes and constitutive activation of Wnt signaling in gastric cancer. *Oncogene* **26:** 4699–4713

Oshima H, Oshima M, Inaba K, Taketo MM (2004) Hyperplastic gastric tumors induced by activated macrophages in COX-2/mPGES-1 transgenic mice. *EMBO J* **23:** 1669–1678

Oshima H, Matsunaga A, Fujimura T, Tsukamoto T, Taketo MM, Oshima M (2006) Carcinogenesis in mouse stomach by simultaneous activation of the Wnt signaling and prostaglandin E_2 pathway. *Gastroenterology* **131:** 1086–1095

Oshima M, Dinchuk JE, Kargman SL, Oshima H, Hancock B, Kwong E, Trzaskos JM, Evans JF, Taketo MM (1996) Suppression of intestinal polyposis in $Apc^{\Delta 716}$ knockout mice by inhibition of cyclooxygenase 2 (COX-2). *Cell* **87:** 803–809

Oshima M, Oshima H, Kitagawa K, Kobayashi M, Itakura C, Taketo M (1995) Loss of *Apc* heterozygosity and abnormal tissue building in nascent intestinal polyps in mice carrying a truncated *Apc* gene. *Proc Natl Acad Sci USA* **92:** 4482–4486

Oshima M, Oshima H, Matsunaga A, Taketo MM (2005) Hyperplastic gastric tumors with spasmolytic polypeptide-expressing metaplasia caused by tumor necrosis factor-α-dependent inflammation in cyclooxygenase-2/microsomal prostaglandin E synthase-1 transgenic mice. *Cancer Res* **65:** 9147–9151

Pikarsky E, Porat RM, Stein I, Abramovitch R, Amit S, Kasem S, Gutkovich-Pyest E, Urieli-Shoval S, Galun E, Ben-Neriah Y (2004) NF-κB functions as a tumour promoter in inflammation-associated cancer. *Nature* **431:** 461–466

Popivanova BK, Kitamura K, Wu Y, Kondo T, Kagaya Y, Kaneko S, Oshima M, Fujii C, Mukaida N (2008) Blocking TNF-α in mice reduces colorectal carcinogenesis associated with chronic colitis. *J Clin Invest* **118:** 560–570

Pull SL, Doherty JM, Mills JC, Gordon JI, Stappenbeck TS (2005) Activated macrophages are an adaptive element of the colonic epithelial progenitor niche necessary for regenerative responses to injury. *Proc Natl Acad Sci USA* **102:** 99–104

Rasola A, Fassetta M, De Bacco F, D'Alessandro L, Gramaglia D, Di Renzo MF, Comoglio PM (2006) A positive feedback loop between hepatocyte growth factor receptor and β-catenin sustains colorectal cancer cell invasive growth. *Oncogene* **26:** 1078–1087

Sharma M, Chuang WW, Sun Z (2002) Phosphatidylinositol 3-kinase/Akt stimulates androgen pathway through GSK3β inhibition and nuclear β-catenin accumulation. *J Biol Chem* **277:** 30935–30941

Sonoshita M, Takaku K, Sasaki N, Sugimoto Y, Ushikubi F, Narumiya S, Oshima M, Taketo MM (2001) Acceleration of intestinal polyposis through prostaglandin receptor EP2 in $Apc^{\Delta 716}$ knockout mice. *Nat Med* **7:** 1048–1051

Suriano G, Vrcelj N, Senz J, Ferreira P, Masoudi H, Cox K, Nabais S, Lopes C, Machado JC, Seruca R, Carneiro F, Huntsman DG (2005) β-Catenin (*CTNNB1*) gene amplification: a new mechanism of protein overexpression in cancer. *Genes Chromosomes Cancer* **42:** 238–246

Taketo MM (2006) Wnt signaling and gastrointestinal tumorigenesis in mouse models. *Oncogene* **25:** 7522–7530

van Noort M, Meeldijk J, van der Zee R, Destree O, Clevers H (2002) Wnt signaling controls the phosphorylation status of β-catenin. *J Biol Chem* **277:** 17901–17905

van de Wetering M, Sancho E, Verweij C, de Lau W, Oving I, Hurlstone A, van der Horn K, Batlle E, Coudreuse D, Haramis AP, Tjon-Pon-Fong M, Moerer P, van den Born M, Soete G, Pals S, Eilers M, Medema R, Clevers H (2002) The β-catenin/TCF-4 complex imposes a crypt progenitor phenotype on colorectal cancer cells. *Cell* **111:** 241–250

Yang L, Lin C, Liu ZR (2006) P68 RNA helicase mediates PDGF-induced epithelial mesenchymal transition by displacing Axin from β-catenin. *Cell* **127:** 139–155